



ISAS - INTERNATIONAL SCHOOL FOR ADVANCED STUDIES

Thesis submitted for the degree

of

"MAGISTER PHILOSOPHIAE"

TIME-DEPENDENT TUNNELING OF WAVE-PACKET
IN A TRANSVERSE MAGNETIC FIELD



CANDIDATE:

XU LIFANG

SUPERVISORS:

Prof. E. TOSATTI

Prof. A. SELLONI

Academic Year 1986/87

Thesis submitted for the degree
of

"MAGISTER PHILOSOPHIAE"

TIME-DEPENDENT TUNNELING OF WAVE-PACKET
IN A TRANSVERSE MAGNETIC FIELD

CANDIDATE:

XU LIFANG

SUPERVISORS:

Prof. E. TOSATTI

Prof. A. SELLONI

Academic Year 1986/87

CONTENTS

CHAPTER 1 : INTRODUCTION

CHAPTER 2 : LANDAU LEVELS IN THE PRESENCE OF
POTENTIAL BARRIER

CHAPTER 3 : SCHEME FOR PROPAGATING THE TIME-DEPENDENT
SCHRODINGER EQUATION

CHAPTER 4 : THE MOTION OF A WAVEPACKET IN A MAGNETIC
FIELD

CHAPTER 5 : TUNNELING THROUGH A POTENTIAL BARRIER IN THE
PRESENCE OF A TRANSVERSE MAGNETIC FIELD

CHAPTER 6 : CONCLUSIONS

REFERENCES

ACKNOWLEDGEMENTS

I would like to express my gratitude to Prof. E.Tosatti and Dr. A.Selloni for their patient instructions and for their invaluable helps during the course of this study.

I am very grateful to Dr.F.Ancilotto for his discussions, for his collaborations, as well as his many helps in computer program.

Chapter 1

INTRODUCTION

The concept of particle tunneling is nearly as old as quantum mechanics itself. Once an electron is represented by a wavefunction, it penetrates into a classically forbidden region, and can tunnel through a reasonably thin potential barrier. In other words, according to quantum mechanics, an electron tunnels through the barrier without requiring enough energy over the top of the barrier[1].

Recently, a great interest has been focussed on the study of tunneling phenomena in semi-conductor GaAs/Ga_{1-x}Al_xAs/GaAs heterostructures not only for the physics of tunneling itself, but also for its implications and potential applications. This is also due to the great development of the Molecular Beam Epitaxy (MBE) technology which allows the fabrication of high-accuracy heterostructures with nearly defect-free barriers and nearly flat interfaces.

In this thesis, we are concerned with tunneling in the presence of a transverse magnetic field. Some of the purposes of our study are to provide a detailed calculation and understanding of barrier traversal time[2,3] and transmission coefficients[4]. Simplistically one might expect the magnetic field to give information about the "velocity" of an electron as it tunnels just as the Lorentz force on a classical electron give a measure of

its velocity. Experimentally people have investigated the influence of a transverse magnetic field on tunneling through low and thick heterostructure barrier to determine the barrier transversal time from a purely static measurement [5]. The tunneling-barrier geometry with an applied transverse magnetic field is shown as figure 1.1:

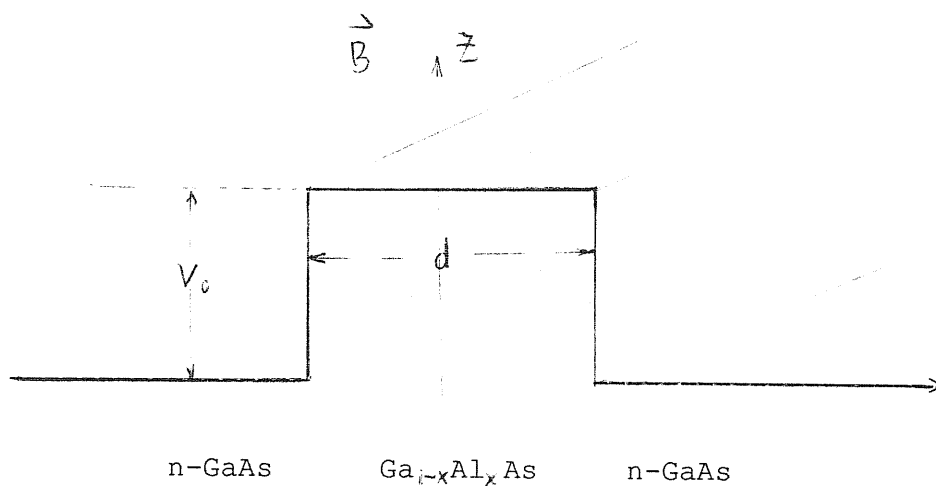


Fig.1.1 The geometry of the heterostructure barrier with applied magnetic field under investigation

Tunneling problems in heterojunction systems have been treated theoretically using effective mass[6] type models, or WKB models[7]. The time-dependent tunneling of wavepackets through heterostructure barriers has attracted considerably less attention than methods based on the stationary Schrodinger equation. The reason for this is obvious: integrating the time-dependent Schrodinger equation forward in time is a quite complicated numerical problem which requires careful programming and large computer resources. Fortunately, several methods for propagating the time-dependent Schrodinger equation have been developed[8]. We need to choose one of them which is suitable to

its velocity. Experimentally people have investigated the influence of a transverse magnetic field on tunneling through low and thick heterostructure barrier to determine the barrier transversal time from a purely static measurement [5]. The tunneling-barrier geometry with an applied transverse magnetic field is shown as figure 1.1:

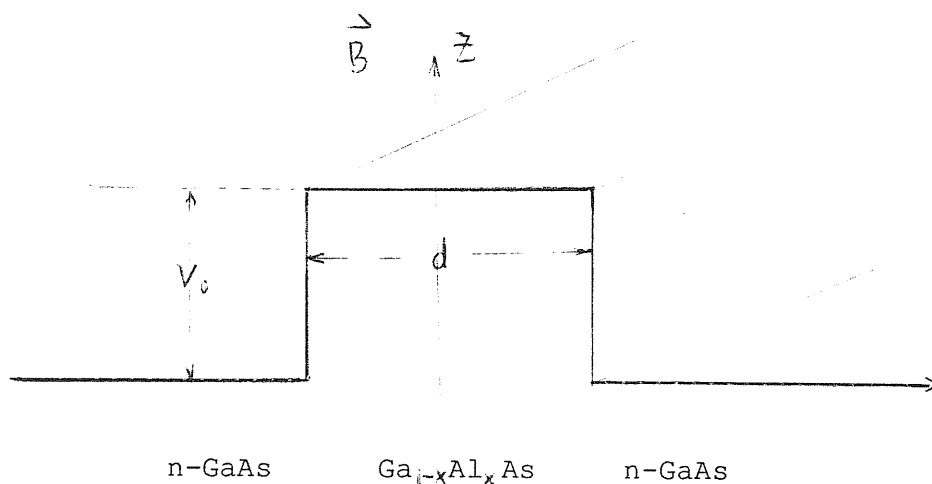


Fig.1.1 The geometry of the heterostructure barrier with applied magnetic field under investigation

Tunneling problems in heterojunction systems have been treated theoretically using effective mass[6] type models, or WKB models[7]. The time-dependent tunneling of wavepackets through heterostructure barriers has attracted considerably less attention than methods based on the stationary Schrodinger equation. The reason for this is obvious: integrating the time-dependent Schrodinger equation forward in time is a quite complicated numerical problem which requires careful programming and large computer resources. Fortunately, several methods for propagating the time-dependent Schrodinger equation have been developed[8]. We need to choose one of them which is suitable to

our problem. In our work the Chebychev polynomial expansion method has been used, which is extremely accurate and efficient, especially for long time intervals.

In this thesis, we shall present numerical solutions of both the time-independent and time-dependent Schrodinger equations in the presence of a magnetic field. The results for the time-independent case have already been discussed in the literature. The reason for discussing them here is just to make the presentation self-contained, and the results for the time-dependent case more easily understandable. The results for the stationary case show that in presence of the barrier the Landau levels become strongly position dependent and oscillate.

The solution of the time-dependent Schrodinger equation for a wavepacket in a magnetic field shows very interesting features (the width σ of the wavepacket smaller than magnetic length $\sqrt{\hbar c / (eB)}$). In absence of the potential barrier, in the first half periodicity the wavepacket moves along the classical circular orbit and spreads during the motion (much less than the free electron case). In the second half periodicity the wavepacket contracts and returns back to the original form. For the particular case of an initial wavepacket with zero velocity, the mean position of the wavepacket does not change in time while the shape of the wavepacket changes periodically as well. We also present the trajectory of a wavepacket tunneling through a potential barrier in a magnetic field. Most of our results for this situation are still very preliminary and will require further investigations.

The thesis is organized in the following way: In chapter 2 the Landau levels of an electron are calculated for both the

case of a thin and a thick barrier by solving the Schrodinger eigenvalue equation. Chapter 3 contains a short review of the scheme we use for propagating the Schrodinger equation. In chapter 4 we present the motion of a wavepacket in a magnetic field. Chapter 5 presents the trajectory of a wavepacket tunneling through a potential barrier in a magnetic field.

Chapter 2

ENERGY LEVELS IN THE PRESENCE OF BOTH
POTENTIAL BARRIER AND MAGNETIC FIELD

Before studying the dynamics of the tunneling of an electron through a potential barrier in the presence of a magnetic field, it is worth to know the static properties of the system. One of the most important information is provided by the energy levels .

With $B \parallel z$ and x the direction perpendicular to the barrier, and using the Landau gauge $A=(0, -Bx, 0)$, the Hamiltonian of the system is given by:

$$\left[-\frac{\hbar^2}{2m^*} \frac{d^2}{dx^2} + \frac{e^2 B^2 x'^2}{2m^*} + V(x) \right] \psi(x) = \left[E + \frac{\hbar^2 k_z^2}{2m^*} \right] \psi(x) \quad (2.1)$$

Since the potential term does not depend on z and y , plane waves are used for the wavefunctions in these directions. The usual substitution $x' = x + \hbar k_y / eB$ has been performed. m^* is the effective mass and all other parameters have their usual meaning.

For $V(x) = \text{constant}$, equation(2.1) represents the well-known harmonic oscillator with equidistant Landau levels [9] having the same energy for all values of $\hbar k_y / eB$, the position of the cyclotron orbit center. This result is due to translational invariance in this case. If $V(x)$ is the potential barrier there is no translational invariance and the eigenvalues will generally depend on the cyclotron orbit center coordinates (centered in the

barrier or out of the barrier). However the equation can be solved numerically[10,11].

The numerical solution of the Schrodinger equation can be carried out by several methods. For instance, the wavefunctions can be expanded in terms of a suitable set of basis functions. The solution of the wave equation is then reduced to a matrix problem, and the linear expansion coefficients can be determined by standard diagonalization methods. The accuracy of this approach is limited by the finite size of basis sets. It is essential to choose each basis function as judiciously as possible.

Alternatively, the stationary Schrodinger equation can be solved by using integration methods such as the Numerov method or the Runge-Kutta method (for one dimensional equations). This is the approach used in this work. In this approach, functions such as the potential $V(x)$ and the wavefunctions are represented by their numerical values at the points of a suitably chosen mesh, and mathematical operations are performed by standard finite difference methods.

2.1)METHOD OF SEARCHING FOR THE EIGENVALUES

Because the Schrodinger equation is an eigenvalue problem, in order to begin the calculation, it is necessary to specify E_i , the starting energy eigenvalue. In this way the eigenvalue problem changes into an ordinary differential equation. The strategy of the Runge-Kutta integration is therefore to integrate from negative infinity to a certain point we have chosen and then integrate from positive infinity to the same point. The logarithmic derivatives of the two wavefunctions (obtained by the integration from both sides) match at this point

only when the energy eigenvalue is correct.

How to search for the correct energy eigenvalues? The wavefunction oscillates in the region where $V(x)-E$ is negative and the number of nodes of this oscillation characterizes the energy level of the system. If there are more nodes than what the energy level calls for, the energy eigenvalue E (the only adjustable parameter in the equation) should be decreased. Once the correct number of nodes is reached one should try to match the logarithmic derivatives of the wavefunction from both sides. Here we shall briefly mention a most commonly used method to match the logarithmic derivatives.

Let u_L and u_R represent solutions obtained from the negative infinity and positive infinity integrations, respectively, and u_L' and u_R' their first derivatives. Also let x_0 be the matching point coordinate, thus the matching condition is

$$(u_L'/u_L)_{x_0} = (u_R'/u_R)_{x_0} \quad (2.2)$$

If the above is not satisfied, one would like to alter it in such a way that a new condition is satisfied.

$$(u_L'/u_L)_{x_0} + \Delta(u_L'/u_L)_{x_0} = (u_R'/u_R)_{x_0} + \Delta(u_R'/u_R)_{x_0} \quad (2.3)$$

This change can be achieved by a variation of the eigenvalue in the Schrodinger equation which will cause a change in the solution. The Schrodinger equations before and after the variation are

$$[(d^2/dx^2) + V + E] u = 0 \quad (2.4)$$

and

$$[(d^2/dx^2) - V + E + \Delta E] (u + \Delta u) = 0 \quad (2.5)$$

Here the V is the total potential term. If the variations E and u are small neglecting second order effects. Eq.(2.5) becomes

$$[(d^2/dx^2) - V + E] \Delta u = -u \Delta E \quad (2.6)$$

Multiplying Eq.(2.6) by u and subtracting from it Eq.(2.4) multiplied by Δu , one has

$$(d/dx) (u \Delta u' - \Delta u u') = u^2 \Delta E \quad (2.7)$$

Integrating the above equation from negative infinity to x_e and from positive infinity to x_o and realizing that

$$u(-\infty) = u(\infty) = \Delta u(-\infty) = u(\infty) = 0, \quad (2.8)$$

One arrives at the two following results:

$$(u_l \Delta u_l' - u_l' \Delta u_l)_{x_e} = \Delta E \int_{-\infty}^{x_e} u_l^2 dx \quad (2.9)$$

and

$$(u_r \Delta u_r' - u_r' \Delta u_r)_{x_o} = -\Delta E \int_{x_o}^{\infty} u_r^2 dx \quad (2.10)$$

It is further noticed that the variation in the logarithmic derivative can be rewritten as

$$\Delta(u'/u) = (\Delta u'/u) - (u' \Delta u / u^2) = (u \Delta u' - u' \Delta u) / u^2 \quad (2.11)$$

Substituting Eqs.(2.9)-(2.11) into Eq.(2.3), one finally obtains the formula for the variation of the eigenvalue

$$\begin{aligned} & [\left(\int_{-\infty}^{x_e} u_l^2 dx / u_l^2(x_e) \right) + \left(\int_{x_o}^{\infty} u_r^2 dx / u_r^2(x_o) \right)] \Delta E \\ & = (u_l' / u_l - u_r' / u_r)_{x_o} \end{aligned} \quad (2.12)$$

On the right-hand side of the above equation the term is named the Wronskin. The equation will insure the continuity of the

logarithmic derivative at the matching point.

For the particular problem at hand Eq.(2.1), the search for the eigenvalues can be made very efficient by exploiting the knowledge of the Landau levels in the absence of the external potential. Because the energy eigenvalues are always larger than $1/2\hbar\omega$, the zero point energy, we started from this trial initial energy as input. The number of the nodes and the Wronskian are calculated at each step when we increase E by a small value ΔE which is chosen according to the desired accuracy. According to Eq.(2.12), the variation of the energy is proportional to the Wronskian. When the absolute value of the Wronskian reaches the local minimum, the energy is the eigenvalue we search for. The number of nodes is the number of the energy level. If it is necessary to increase the accuracy, one can decrease ΔE starting from a value slightly smaller than the energy eigenvalue obtained previously.

2.2) RESULTS AND ANALYSIS

The results of the above described calculations are shown in Figs.2.1 and 2.2 which refer to a thin barrier and to a thick barrier respectively. The interesting feature which appears is that in presence of the barrier the Landau levels become strongly position dependent and oscillate.

For the thin barrier the number of minima in the oscillation of the energy level is the same as the number of the nodes of the wavefunction corresponding to this energy level. As mentioned before the Schrodinger equation(2.1) only depends on the relative distance of the positions of the cyclotron orbits center and the barrier center. When the barrier center is at the place of the nodes of the electron wavefunction in the magnetic

field, the influence of the barrier on the energy is small. This corresponds to the minima of the oscillation of the Landau level. The number of nodes of the wavefunction decides the number of minima of the Landau level. On the other hand when the barrier is placed where the wavefunction has the maximum or minimum, the effect of the barrier on the wavefunction is large corresponding to the maxima of the energy level.

For the thick barrier the number of minima of the energy levels do not correspond to the number of nodes of the wavefunction any longer. The higher the energy level is, the more nodes the wavefunction has, the shorter the distance between two neighbouring nodes is. The thick barrier not only influences the nodes or the extrema, but influences both the nodes and the extrema simultaneously. In this case we must take into account the total effect on the nodes and extrema. This effect shows up for instance in the levels ≥ 7 of Fig.2.2.

THIN POTENTIAL BARRIER

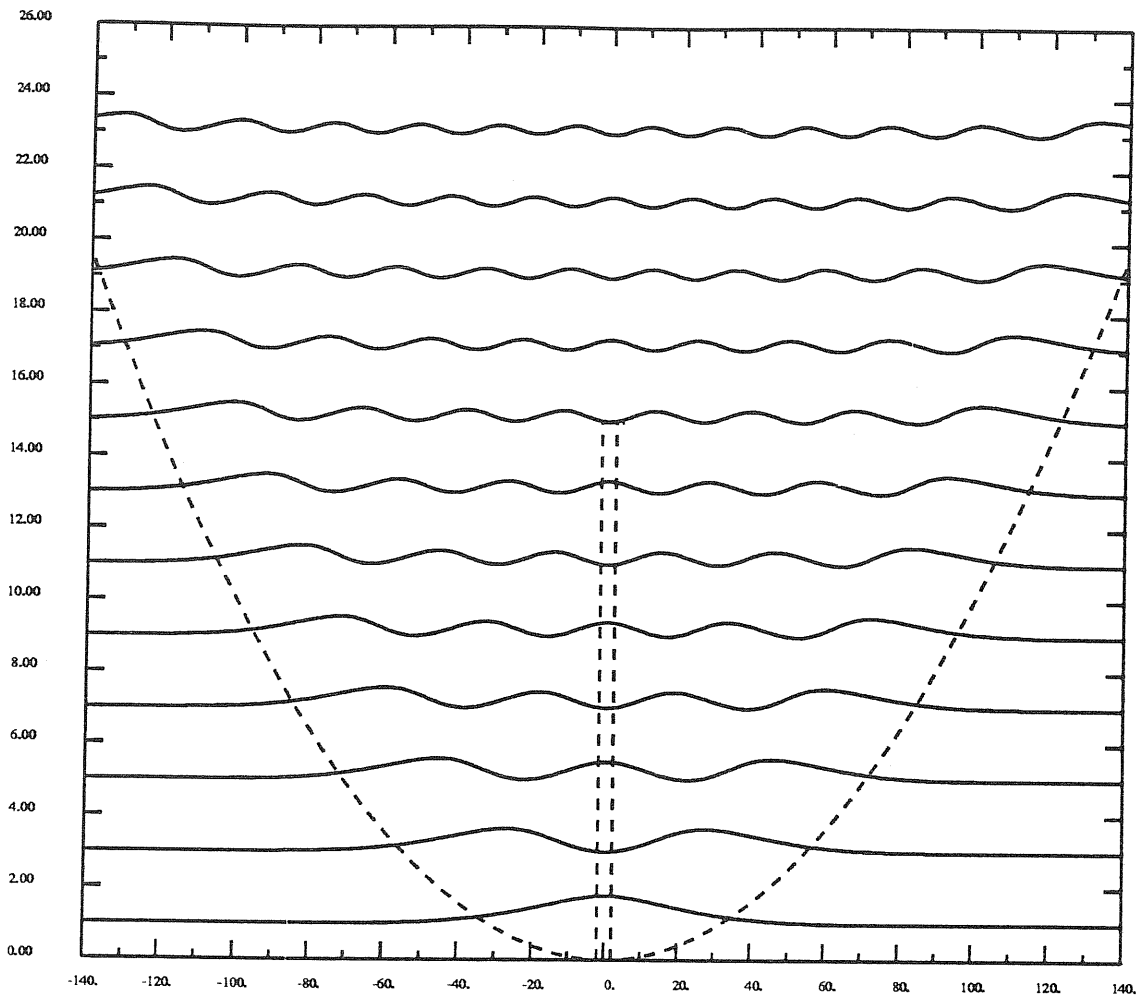


Fig.(2.1) Landau levels in the presence of a thin potential barrier. The number of minima of the Landau levels corresponds to the number of nodes of the wavefunction. (The dashed curves indicate the parabolic potential from the magnetic field and squared potential barrier).

LOW AND THICK POTENTIAL BARRIER

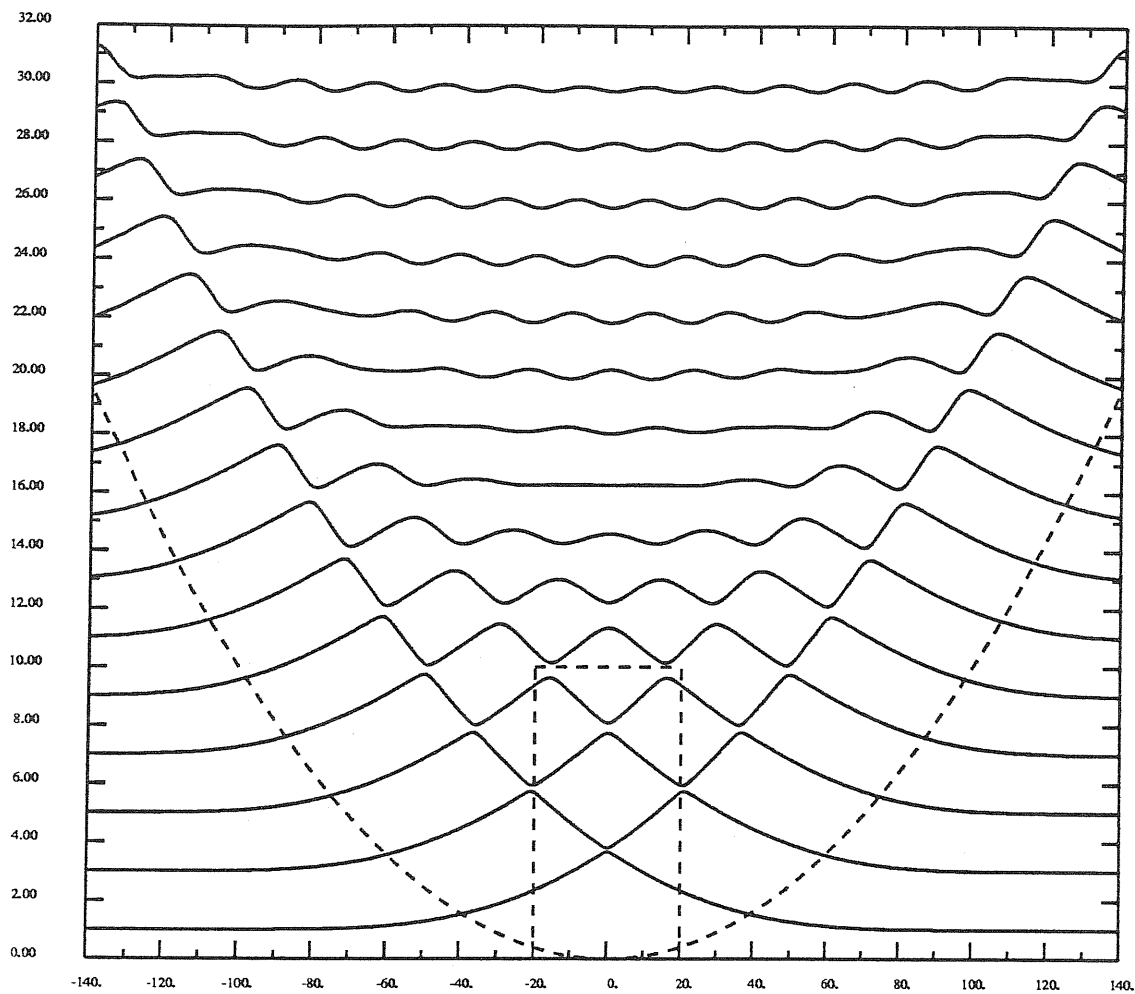


Fig.(2.2) Landau levels in the presence of a low and thick potential barrier. The number of minima of the Landau levels does not correspond to the number of nodes of the wavefunction any longer. (The dashed curves indicate the parabolic potential from the magnetic field and squared potential barrier).

Chapter 3

SCHEME FOR PROPAGATING THE TIME-DEPENDENT SCHRODINGER EQUATION

The scheme chosen for solving the time dependent Schrodinger equation is based on a Chebychev polynomial expansion of the time evolution operator $U=\exp(-iHt)$. Combined with the Fourier method for calculating the kinetic operator in the Hamiltonian, the scheme is extremely accurate. The advantage of the scheme is that the time interval t is not limited [8,12].

For tunneling calculations, grid methods can be extremely useful. These methods are accurate and modular in structure. The numerical procedure can be divided in four steps: a)Setting an initial wave function on the grid. b)Establishing a method to calculate the Hamiltonian operation. C)Propagating the wavefunction in time. d)Analyzing the final propagated wavefunction. Because of this modular structure each step can be done separately by a variety of techniques. Accuracy can be controlled in each step separately. Tunneling problems can be easily treated by these methods. Cartesian coordinates can be used in these methods.

3.1) DISCUSSION OF GRID METHODS FOR WAVEFUNCTION REPRESENTATION

In quantum mechanics the state of the system is

represented by the wavefunction. All observable information on the system is extracted from this wavefunction. The time evolution of the wavefunction is governed by the Schrodinger equation:

$$i\hbar \frac{\partial \psi}{\partial t} = H \psi \quad (3.1)$$

A numerical construction of a solution to the time-dependent equation follows the three stages: First the wavefunction is represented on a discrete grid (values of between grid points are obtained by interpolation). Secondly, the Hamiltonian operator:

$$H = \frac{p^2}{2m} + V \quad (3.2)$$

and its operation on ψ , $H\psi$ are calculated. Thirdly, a time propagation scheme is constructed which transforms the initial wavefunction to the final one. Different numerical methods can be classified by the way each of these steps is carried out.

Wavefunctions pertinent to our interest are continuous functions extended in space. All grid methods represent such a function at a set of discrete sampling points. The values of the wavefunction between sampling points is recovered by interpolation. In grid methods, the size and shape of the grid have to be adapted to the physical problem. For two-dimensional tunneling calculations, rectangular grids with uniform sampling points have been used. Although non-uniform grids may be advantageous in special cases, it is not suitable for our problem. The size of the grid must be large enough to contain the wavefunctions from the initial state to the final one.

Boundary conditions of the grid are an important issue. Since we use the Fourier method to calculate spatial derivatives,

we are restricted to periodic boundary conditions. There is no periodic property in our tunneling problem. The space should be chosen large enough to contain the wavefunctions inside and at the far end of the grid the wavefunctions are closed to zero.

3.2) THE INITIAL WAVEFUNCTION

After the grid has been set up, the initial wavefunction has to be placed on it. Because of the finite size of the grid the wavefunction has to be semi-localized. The wavefunctions are localized on the surface perpendicular to z , the direction of the magnetic field B , whereas they form a plane wave in this direction. In fact this is a two-dimensional problem. Usually the localization in the x - y plane is done by choosing a Gaussian wavepacket.

$$\psi_0(x, y) = [2\pi\sigma]^{\frac{1}{2}} \exp\left\{-\frac{(x-x_0)^2 + (y-y_0)^2}{4\sigma^2}\right\} + \frac{i\langle p_x \rangle x + i\langle p_y \rangle y}{\hbar} \exp[ik_z z] \quad (3.3)$$

This form of the wavepacket corresponds to the minimum value of the uncertainty product. σ is the width of wavepacket, x_0 and y_0 are the initial average positions in x , y , respectively, $\langle p_x \rangle$, $\langle p_y \rangle$ are the momenta in the x and y directions, k_z is wavenumber in the z direction.

3.3) HAMILTONIAN OPERATION WITH THE FOURIER METHOD

The Hamiltonian operation can be partitioned into potential and kinetic parts. Because the potential energy operator is a local operator in coordinate space its operation is the simple multiplication at each spatial grid point. For a two-dimensional problem where i is the spatial index in x and j in y

the operation becomes:

$$V(i, j) \Psi(i, j) \quad (3.4)$$

The main difficulty in the Hamiltonian operation arises from the kinetic energy operator because of its non-local character. However a local operation of the kinetic energy can be calculated in K space. The transformation from the coordinate space to the momentum space is the Fourier transform. At this step the K space wavefunction is multiplied by $-iK$ for operation \hat{V} in coordinate space. The operation is completed by transforming back to coordinate space using an inverse Fourier transform. The numerical procedure is as follows: A) Transform $\Psi(i, j)$ to $\tilde{\Psi}(n, m)$ in K space by a two-dimensional discrete Fourier transform. B) Multiply $\tilde{\Psi}(n, m)$ by $-ik_x$ and $-ik_y$, for each derivative operators $\partial/\partial x$, and $\partial/\partial y$. C) Transform the result of B to coordinate space by an inverse 2-D Fourier transform. Numerical efficiency of the method is the result of the Fast Fourier Transform (FFT) algorithm [13,14]. For this algorithm numerical effort grows as $O(N \ln N)$ where N is the number of grid points.

An important advantage of the method is that the commutation relations of quantum mechanics, $[P, f(x)] = i\hbar f'(x)$ are preserved in the discrete representation. This means that the discrete Hilbert space used for modeling the problem has the same commutation relations as the continuous Hilbert space and the correct operator algebra is mapped to the discrete world.

ERROR ANALYSIS

Errors in the Fourier method are a result of two sources: a) The grid is not large enough to contain the wavefunction or does not match the periodic boundary conditions. For instance,

the average momentum should satisfy the relation: $\langle K \rangle L = 2\pi M$, where L is the total length of the grid and M is an integer.

b) The grid is not dense enough which results in under sampling of high momentum components of the wavefunction. For Gaussian type wave functions, the convergence of the method is exponential when increasing the grid size or grid density. Practically when constructing a grid care should be taken that the maximum momentum in the wave function does not exceed: $p_{\max} < \pi \hbar / \Delta x$, where the $\Delta x = L/N$, N being the number of the grid points.

3.4) TIME PROPAGATION SCHEME

The next step in the grid method is to propagate the wavefunction in time. The general solution of the Schrodinger equation has the form:

$$\psi(t+dt) = \exp(-iHdt/\hbar) \psi(t). \quad (3.5)$$

For grid methods time propagation schemes have to be simple because they are applied on each grid point. This fact usually rules out predictor-correct variable step integrators.

For solving the time-dependent Schrodinger equation, we chose the CHEBYCHEV TIME PROPAGATION METHOD which can eliminate the error in propagation almost completely [12]. The strategy chosen for the propagation scheme is to expand the evolution operator $U = \exp(-iHdt/\hbar)$ in a polynomial series in the operator: $-iHdt/\hbar$. The problem then becomes a choice of the best polynomial approximation for the series. It has been shown that this problem reduces to approximating the scalar function e^z by a polynomial expansion where z belong to the domain which includes all the eigenvalues of the operator $-iHdt/\hbar$. It is known that the best approximation is achieved by an expansion based on the

complex Chebychev polynomial Φ_k . (the reason is the uniform character of the complex Chebychev polynomials in distributing the error in the interval $[-i, i]$.) These polynomials are a complex version of the Chebychev polynomials and they are defined as:

$$\Phi_k(w) = i^k T_k(-iw), \quad w \in [-i, i] \quad (3.6)$$

and the T_k are the Chebychev polynomials of the first kind. The Φ_k are orthogonal on the imaginary interval $[-i, i]$ with respect to the following inner product:

$$\langle f, g \rangle = -i \int_{-i}^i \frac{f(w)g^*(w)}{\sqrt{1-|w|^2}} dw. \quad (3.7)$$

The domain of the eigenvalues of the Hamiltonian $H = P^2/2m + V$ depends on the discretization scheme. The domain of the eigenvalues can be estimated as follows. The maximum kinetic energy is $P_{\max}^2/2m$. If the minimum of the potential (represented on the grid) is V_{\min} and its maximum V_{\max} , the range of the eigenvalues of H is

$$\lambda \in \left\{ V_{\min}, V_{\max} + \frac{\hbar^2 \pi^2}{2m(\Delta x)^2} \right\}$$

Where Δx is the spatial grid interval in one dimension. The scalar function z is chosen to be in the range of $i\lambda dt$. Defining

$$R = dt \left(\frac{\hbar^2 \pi^2}{2m \Delta x^2} + \frac{V_{\max} - V_{\min}}{2\hbar} \right), \quad G = V_{\min} dt / \hbar \quad (3.8)$$

and

$$w = (z - iR - iG) / R \quad (3.9)$$

one obtains:

$$e^z = e^{i(R+G)Rw} e^{Rw}, \quad w \in [-i, i]. \quad (3.10)$$

At this step e^z is expanded into the Chebychev series:

$$e^z = \sum_{k=0}^N a_k \Phi_k(w), \quad (3.11)$$

where:

$$a_k = -i e^{i(R+G)} \int_{-i}^i \frac{e^{R\omega} \Phi_k(\omega)}{\sqrt{1-|\omega|^2}} d\omega = e^{i(R+G)} C_k J_k(R) \quad (3.12)$$

and $C = 1$ for $k=0$ and $C = 2$ for $k > 0$. J_k are Bessel functions of the first kind of order k . The high accuracy of this expansion can be traced to the fact that when k is greater than R , $J(R)$ goes to zero exponentially fast. Thus the degree N of the expansion has to be at least R . In this work N was chosen to be αR where $\alpha > 1$. The values of α depends on the degree of accuracy needed and can be chosen to bring errors below the accuracy of the computer. The propagation scheme is obtained by substituting $-iHdt/h$ for z in (3.11) and using (3.12)

$$\hat{U}(dt) = \sum_{k=0}^N a_k \Phi_k\left(-\frac{iHdt}{hR}\right) \quad (3.13)$$

where the Chebychev polynomials in the operator $iHdt/hR$ are computed by the recurrence relation satisfied by the polynomials $\Phi_k(X)$

$$\Phi_k(X) = 2X\Phi_{k-1}(X) + \Phi_{k-2}(X)$$

and

$$\Phi_0(X) = 1, \quad \Phi_1(X) = X,$$

where X is the operator $-iHdt/hR$ and where H is shifted by $-hR/(2dt) + V_{min}$, in order to distribute the eigenvalues in the interval $[-i, i]$. As a result $R + G = 0$ in eqs. (3.11) - (3.13).

The basic algorithm is used as a one step propagator obtaining the solution at the final time $t + dt$ directly from the

initial data, or as a marching scheme if one is interested in intermediate results. The size of the time step dt depends only on the information one wants to get out of numerical procedure. R and the order N are determined accordingly. The refinement of the scheme is then based on increasing the order of the expansion and not by decreasing the time step.

ERROR ANALYSIS

In the above Chebychev propagation scheme errors are both in phase and in energy. The energy and norm are not conserved because the Chebychev scheme is not unitary. This means that the error can also be estimated by the deviation of the energy and norm of the propagated wave function. The errors are distributed uniformly in the domain of the eigenvalues. Because of the exponential decay of the Bessel expansion coefficients this error can be chosen to be lower than the numerical precision of the computer by using enough expansion coefficients.

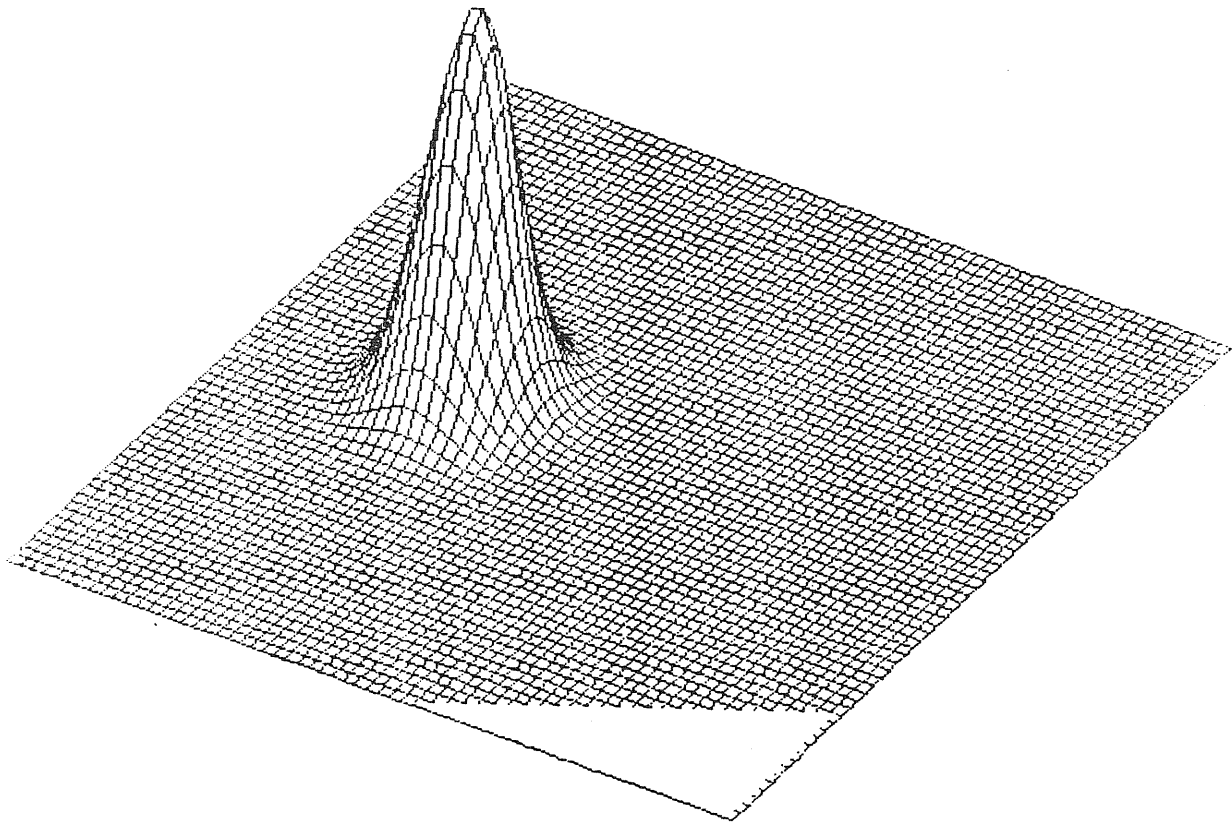


Fig. 3.1

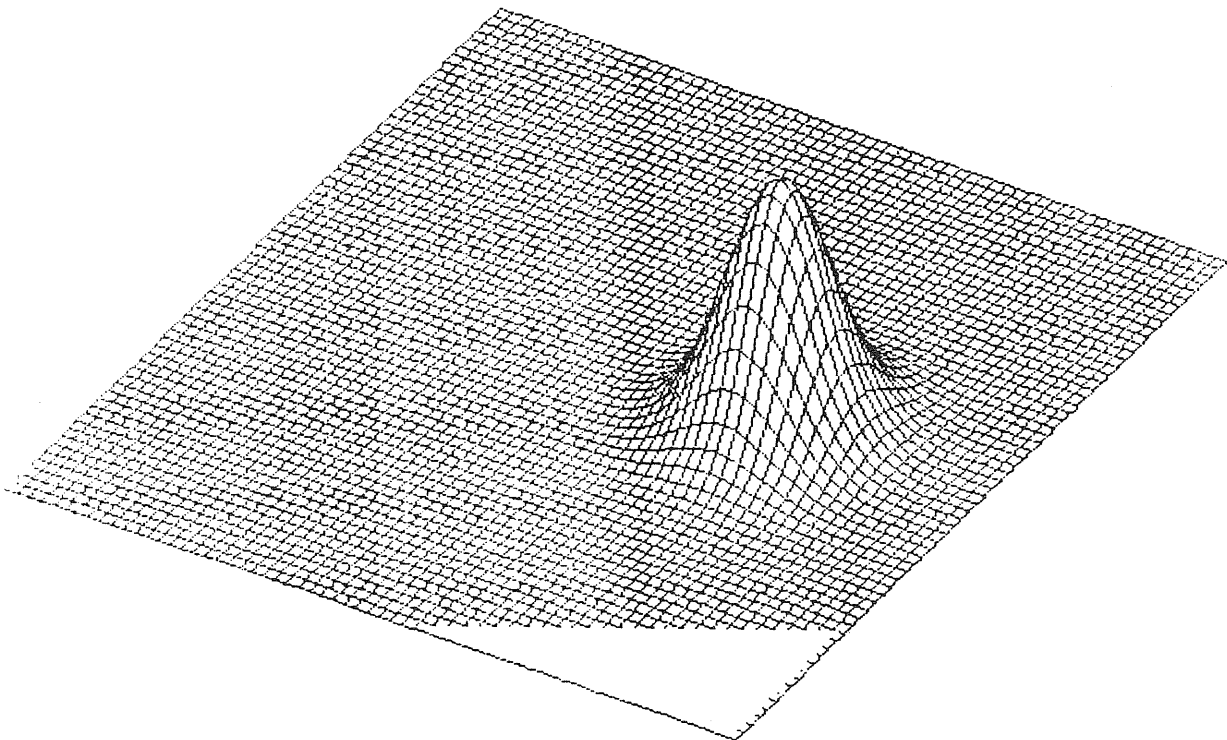


Fig. 3.2

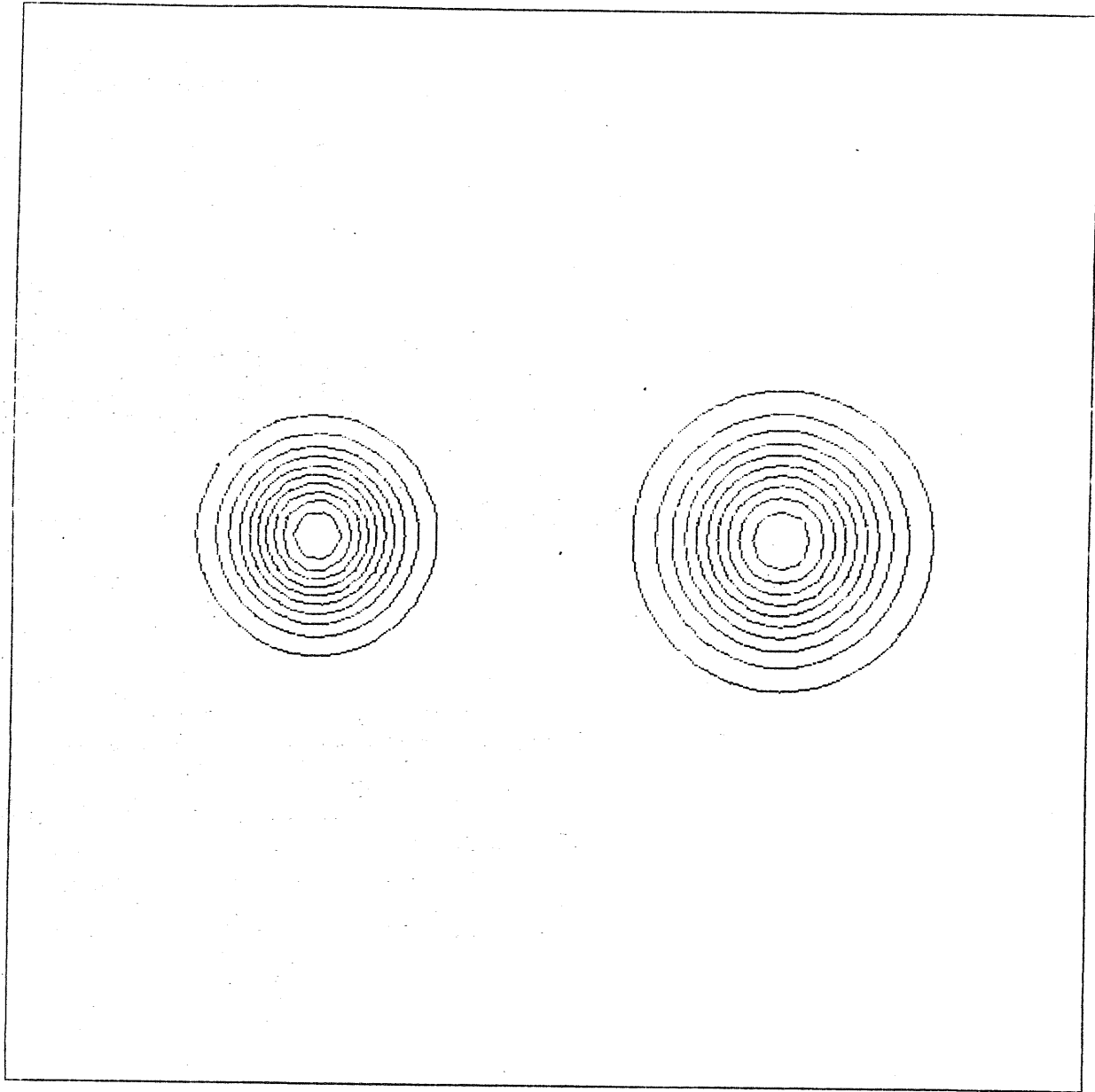


Fig. 3.3

Fig. (3.1)-(3.3) A free wavepacket propagation in time. It spreads fast during the motion.

Chapter 4

THE MOTION OF A WAVEPACKET IN A MAGNETIC FIELD

In this chapter we calculate the motion of a wavepacket in a magnetic field by using the Chebychev polynomial expansion scheme presented in the previous chapter to solve the time-dependent Schrodinger equation. We find that the trajectories are classical circular orbits and obey the Ehrenfest equation and that the wavepackets are confined during the motion.

4.1) EHRENFEST'S EQUATION FOR AN ELECTRON IN A MAGNETIC FIELD

The Ehrenfest Theorem gives the law of motion of the mean values of the coordinates q and the conjugate momenta p of a quantum system. It states that the equations of motion of these mean values are formally identical to the Hamilton equations of Classical Mechanics, except that the quantities which occur on both sides of the classical equations must be replaced by their average values[15].

Consider the Schrodinger equation and the complex conjugate equation:

$$i\hbar \frac{\partial \psi}{\partial t} = H\psi, \quad i\hbar \frac{\partial \psi^*}{\partial t} = -(H\psi)^* \quad (4.1)$$

If ψ is normalized to unity at the initial instant, it remains normalized at any later time. The mean value of a given observable A is equal at any instant to the scalar product:

$$\langle A \rangle = \langle \psi, A \psi \rangle = \int \psi^* A \psi dt, \quad (4.2)$$

and one has

$$\frac{d}{dt} \langle A \rangle = \left\langle \frac{\partial \psi}{\partial t}, A \psi \right\rangle + \left\langle \psi, A \frac{\partial \psi}{\partial t} \right\rangle + \left\langle \psi, \frac{\partial A}{\partial t} \psi \right\rangle \quad (4.3)$$

The last term of the right-hand side, $\langle \partial A / \partial t \rangle$, is zero if A does not depend upon the time explicitly.

Taking into account the Schrodinger equation and the hermiticity of the Hamiltonian, one has

$$\begin{aligned} \frac{d}{dt} \langle A \rangle &= -\frac{i}{\hbar} \langle H \psi, A \psi \rangle + \frac{i}{\hbar} \langle \psi, A H \psi \rangle + \left\langle \frac{\partial A}{\partial t} \right\rangle \\ &= -\frac{i}{\hbar} \langle \psi, [A, H] \psi \rangle + \left\langle \frac{\partial A}{\partial t} \right\rangle. \end{aligned} \quad (4.4)$$

Hence we obtain the general equation giving the time-dependence of the mean value of A :

$$i\hbar \frac{\partial}{\partial t} \langle A \rangle = \langle [A, H] \rangle + i\hbar \left\langle \frac{\partial A}{\partial t} \right\rangle. \quad (4.5)$$

Let q_1, \dots, q_r be the (Cartesian) coordinates of the position; p_1, \dots, p_r their conjugate momenta, and $H(q_1, \dots, q_r; p_1, \dots, p_r)$ the Hamiltonian of the system.

The equation can be written,

$$i\hbar \frac{\partial}{\partial t} \langle q_i \rangle = \langle [q_i, H] \rangle \quad (4.6)$$

$$i\hbar \frac{\partial}{\partial t} \langle p_j \rangle = \langle [p_j, H] \rangle.$$

and using commutators,

$$[q_i, H] = \frac{\partial H}{\partial p_i}, \quad [p_j, H] = -\frac{\partial H}{\partial q_j}, \quad (4.7)$$

The results are:

$$\frac{d}{dt} \langle q_i \rangle = \left\langle \frac{\partial H}{\partial p_i} \right\rangle, \quad (i=1, 2, \dots, r) \quad (4.8)$$

$$\frac{d}{dt}\langle p_j \rangle = -\left\langle \frac{\partial H}{\partial q_j} \right\rangle, \quad (j=1, 2, \dots, r)$$

It is generally not correct to state that the mean values $\langle q_i \rangle$ and $\langle p_j \rangle$ follow the laws of Classical Mechanics. The derivatives with respect to time of the classical quantities q_i and p_j are well-defined functions $\partial H / \partial p_i$, $-\partial H / \partial q_i$ of these quantities. The values taken by these quantities in the course of time can be exactly derived from their initial values. According to equation (4.1) on the other hand, the derivatives $d\langle q_i \rangle / dt$, $d\langle p_j \rangle / dt$ are equal to certain average values whose calculation generally must know the wavefunction $\Psi(t)$. The mean values $\langle q_i \rangle$, $\langle p_j \rangle$ do not follow the classical laws of motion unless one can replace the mean values in (4.1) of the functions of the right-hand sides by the functions of the mean values

$$\left\langle \frac{\partial}{\partial p_i} H(q_1, \dots, q_r; p_1, \dots, p_r) \right\rangle \text{ by } \frac{\partial}{\partial p_i} (H(\langle q_1 \rangle, \dots, \langle q_r \rangle; \langle p_1 \rangle, \dots, \langle p_r \rangle)) \quad (4.9)$$

$$\left\langle \frac{\partial}{\partial q_j} H(q_1, \dots, q_r; p_1, \dots, p_r) \right\rangle \text{ by } \frac{\partial}{\partial q_j} (H(\langle q_1 \rangle, \dots, \langle q_r \rangle; \langle p_1 \rangle, \dots, \langle p_r \rangle))$$

This replacement is rigorously justified only if the Hamiltonian is polynomial of the second degree with respect to q 's and the p 's.

Let us now consider the case of an electron in a magnetic field. If we choose the SYMMETRY gauge $A = (By/2, -Bx/2, 0)$ the Hamiltonian can be written as:

$$H = P_x^2 / (2m) + P_y^2 / (2m) - 1/2w(xP_y - yP_x) + 1/8mw^2(x^2 + y^2). \quad (4.10)$$

Here $w = eB / (mc)$. The form satisfies the condition that the Hamiltonian is quadratic with respect to x, y and p_x, p_y .

Substituting the Hamiltonian (4.10) into the equation

(4.1), the calculation is easily performed and gives

$$\left. \begin{aligned} \dot{x} &= P_x/m + wy/2 \\ \dot{y} &= P_y/m - wx/2 \end{aligned} \right\} \quad (4.11)$$

and

$$\left. \begin{aligned} \dot{P}_x &= wP_y/2 - mw^2x/4 \\ \dot{P}_y &= -wP_x/2 - mw^2y/4 \end{aligned} \right\} \quad (4.12)$$

Eliminating the variable P_x and P_y from Eqs. (4.11) and (4.12), we obtain:

$$\left. \begin{aligned} \ddot{x} &= w\dot{y} \\ \ddot{y} &= -w\dot{x} \end{aligned} \right\} \quad (4.13)$$

which gives:

$$\left. \begin{aligned} \ddot{x} + w^2x &= 0 \\ \ddot{y} + w^2y &= 0 \end{aligned} \right\} \quad (4.14)$$

The solutions can be written down immediately:

$$x = C_1 + A_1 \cos(wt) + B_1 \sin(wt) \quad (4.15)$$

$$y = C_2 + A_2 \cos(wt) + B_2 \sin(wt)$$

Using the initial conditions, we get:

$$A_1 = -B_2 = -P_y^0 / (mw) + x_0 / 2 \quad (4.16)$$

$$A_2 = B_1 = P_x^0 / (mw) + y_0 / 2$$

$$C_1 = P_y^0 / (mw) + x_0 / 2$$

$$C_2 = -P_x^0 / (mw) + y_0 / 2$$

Eliminating the time t , we get

$$(x - C_1)^2 + (y - C_2)^2 = (A_1^2 + A_2^2)^{1/2} \quad (4.17)$$

This is the equation for a circular orbits with the center coordinates (C_1, C_2) and radius $R = (A_1^2 + A_2^2)^{1/2}$.

4.2) VELOCITY OPERATOR IN THE PRESENCE OF A MAGNETIC FIELD AND THE EQUATION OF MOTION

The velocity operator in the presence of a magnetic field is not simply the derivative operation with respect to coordinates $\vec{P}/m = -i\hbar \vec{\nabla}/m$. The correct formula is :

$$\vec{v} = (\vec{P} + e\vec{A}/c)/m \quad (4.18)$$

Here the \vec{A} is the vector potential $\vec{B} = \vec{\nabla} \times \vec{A}$.

Using the SYMMETRIC gauge $\vec{A} = (By/2, -Bx/2, 0)$, the velocity operator can be written:

$$v_x = (P_x + By/2)/m = P_x/m + wy/2 \quad (4.19)$$

$$v_y = (P_y - Bx/2)/m = P_y/m - wx/2$$

Which has the exact form as Eqs.(4.11). Suppose the initial values are P_x^0, P_y^0 and x_0, y_0 , then the initial velocity is

$$v = (v_x^2 + v_y^2)^{1/2} = [(P_x^0/m + wy_0/2)^2 + (P_y^0/m - wx_0/2)^2]^{1/2} \quad (4.20)$$

The radius of the orbit is:

$$R = v/w = [(P_x^0/(mw) + y_0/2)^2 + (P_y^0/(mw) - x_0/2)^2]^{1/2} \quad (4.21)$$

The coordinates of the center of the orbit are easy to calculate. The equation of the straight line perpendicular the initial velocity direction and passing through the initial position x_0, y_0 ,

is:

$$y - y_0 = - \frac{U_x^0}{U_y^0} (x - x_0) \quad (4.22)$$

The coordinates of the center of orbit are on this line. We have

$$\left\{ \begin{array}{l} y_c - y_0 = - \frac{P_x^0}{P_y^0} (x_c - x_0) \\ (x_c - x_0)^2 + (y_c - y_0)^2 = R^2 \end{array} \right. \quad (4.23)$$

The solution of the Eq. (4.23) is:

$$x_c = P_y^0 / (mw) + x_0 / 2 \quad (4.24)$$

$$y_c = -P_x^0 / (mw) + y_0 / 2$$

There are exactly the same values as those obtained from the solution of the Ehrenfest equation.

4.3) TECHNICAL ASPECTS

UNITS: The choice of the units is an important issue in the calculation. A suitable unit can simplify the formula, decrease the errors and storage. Atomic units are usually used in theoretical calculations. It is more convenient to choose the units of the order of the physical quantities in the problem. In our work, the units are chosen as follows:

TIME: picosecond [ps]

LENGTH: angstrom [A]

ENERGY: electron volt [eV]

MAGNETIC FIELD: tesla [T]

GRID SIZE: The grid size (i.e. the ratio between the space size and the number of grid points L/N) must be small

enough to give a sufficiently good representation of the wavefunction at all times. Usually if the grid size is dense for the initial wavepacket, it will be dense enough at any instant. A criterion to decide if the grid size is suitable, is to check the normalization of the initial wavepacket. The calculation increases as $N \ln(N)$ in FFT method, where N is the number of grid points.

TIME INTERVAL: As mentioned before, the advantage of the CHEBYCHEV scheme is that the time interval T is not limited, T can be increased by increasing the order of the expansion. If one calculates the time evolution from t_0 to t_1 , and then from t_1 to t_2 , the results are exactly the same as going directly from t_0 to t_2 .

ACCURACY: Accuracy is the most important point in the numerical calculation. Because the Chebychev scheme is not unitary, the norm and energy are not conserved, the error are estimated by the deviation of the norm and the energy of the propagated wavefunction. The accuracy in our calculation is at least order of 10^{-3} . If higher accuracy is needed, one only needs to increase the number of expansion terms.

4.4) RESULTS AND DISCUSSION

The results we calculated are shown in Figs.(4.1)-(4.10). For convenience, the initial wavepacket is located at the origin because the velocity $\langle v \rangle$ is equal to $\langle P \rangle / m$ at this point. The initial wavepacket has the symmetric form :

$$\psi_0(x, y) = [2\pi\sigma^2]^{-1/2} \exp\left\{-\left(\frac{(x-x_0)^2 + (y-y_0)^2}{4\sigma^2}\right) + \frac{i\langle P_x \rangle x + i\langle P_y \rangle y}{\hbar}\right\} \exp[ik_z z] \quad (4.25)$$

Here the symmetry gauge $A=(By/2, -Bx/2, 0)$ is used, and the Hamiltonian is the same as in Eq.(4.10)

$$H = P_x^2/(2m) + P_y^2/(2m) - 1/2w(xP_y - yP_x) + 1/8mw^2(x^2 + y^2).$$

The wavepacket moves along the cyclotron orbit as we expected. The interesting features are that during the first half periodicity if the width of wavepacket σ_c is smaller than the magnetic length $L_B = (hc/(eB))^{1/2}$, the wavepacket spreads. The spread reaches the maximum at half periodicity. In the second half periodicity the wavepacket contracts back to the original form (both the position and the shape). see Figs.(4.1)-(4.6). If the width of wavepacket σ_c is equal to the magnetic length L_B , the wavepacket does not change the shape during the motion. see Fig.(4.7). If σ_c is larger than the magnetic length L_B the wavepacket contracts during the first half periodicity. The contract reaches the maximum at half periodicity. And then the wavepacket spreads back to the initial form. see Fig.(4.8). These properties remain in the case of a wavepacket with zero velocity. The mean position of the wavepacket remains always the same in time, while the shape of the wavepacket changes periodically. Since the frequency $w=eB/(mc)$ is independent of the velocity of the wavepacket. The velocity only influences the radius of the cyclotron orbit according to the formula $R=v/w$.

The motion of a wavepacket in a magnetic field is periodical. The periodicity can be roughly explained as follows: suppose that the initial wavepacket can be expanded into the complete set of eigenfunctions of the Hamiltonian and that the eigenvalues of the Hamiltonian have the form of $(N+1/2)hw$, N being any integer. When the time evolution operator $U=\exp(-iHt/h)$ is applied to the eigenfunctions, It simply gives the values

$\exp(-iE_N t/\hbar)$. If t is equal to T , the result is $\exp(-i(N+1/2)2\pi)$. Here we have used the relation $\omega T=2\pi$. The final wavefunction differ only by the phase shift $\exp(-i\pi)$ from the initial one.

The shape of a wavepacket changes during the first half periodicity. It can be understood by comparing with the case of free wavepacket propagation in the same time interval, shown in Fig.(4.9). It spreads much faster. This means that the wavepacket is confined by magnetic field. The confinement becomes stronger with increasing magnetic field. The wavepacket with width spreads when $\sigma_0 < L_B$, Wavepacket keeps the shape when $\sigma_0 = L_B$, and wavepacket contracts when $\sigma_0 > L_B$. Here $L_B = (\hbar c / (eB))^{1/2}$ is magnetic length. For the second half periodicity one can imagine that this is the inverse process of the first half periodicity, because the wavepacket should be back to the original form in a full periodicity.

According to the analogue of one dimensional case that a wavepacket moves in a parabolic potential, we get the formula of the width of wavepacket in time:

$$\sigma_t = \sigma_0 (\cos(\omega t/2) + R^2 \sin^2(\omega t/2))$$

Here σ_0 is initial width of wavepacket, $R = (\sigma_0 / L_B)^2$.

If the Landau gauge is employed, the Hamiltonian is:

$$H = P_x^2 / (2m) + P_y^2 / (2m) - \omega x P_y + 1/2 m (\omega x)^2$$

The time evolution of the same initial wavepacket, which is used in the case of the symmetry gauge, is shown in Fig.(4.10). One can remark that, while the trajectory of the mean position is the same for the two gauges, the shape of the wavepacket in the Landau gauge is does not keep circular with respect to the

symmetry gauge. These differences can be understood as follows: The velocity operator $v=(P-eA/c)/m$ in Landau gauge to this initial wavepacket is not rotation invariance. If one wants to use Landau gauge, one can perform a gauge transformation from the symmetry gauge to the Landau gauge. The scalar function of the gauge transformation is $Bxy/2$. Therefore the initial wavefunction should be multiplied by the phase factor $\exp(iBxy)$. And then the velocity operator V is rotation invariance. The results will then be identical for the two gauges.

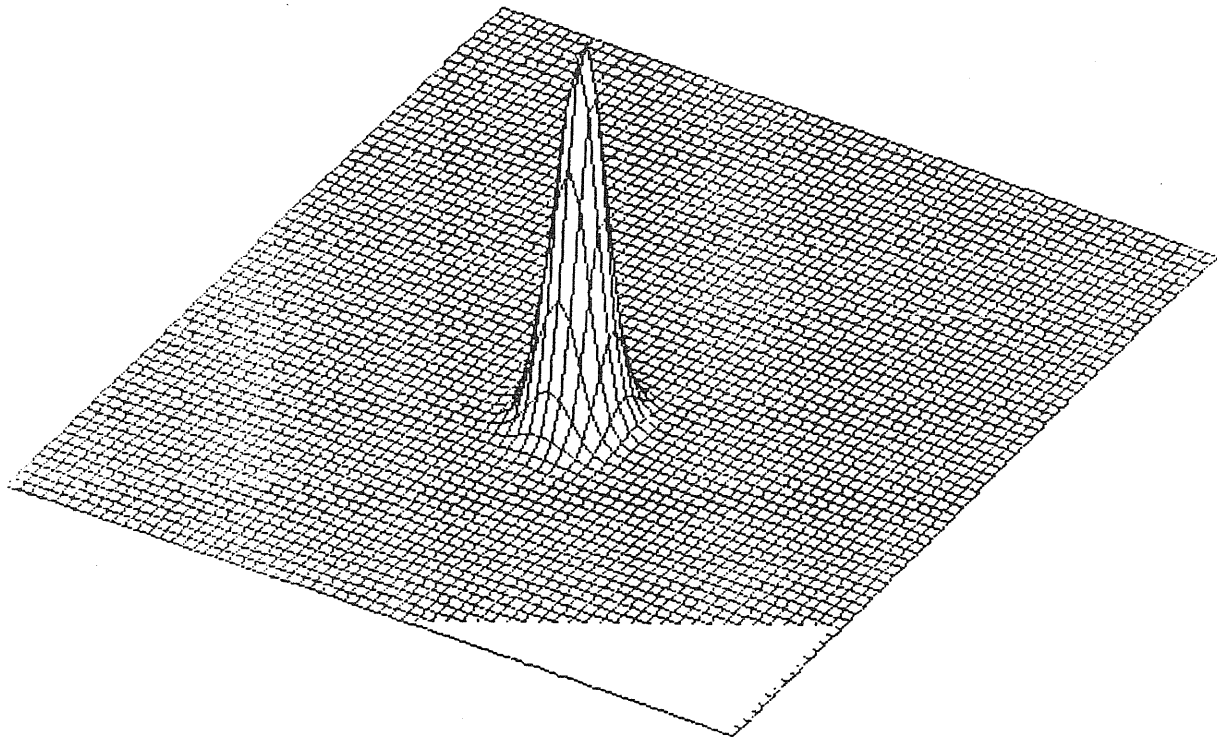


Fig. 4.1

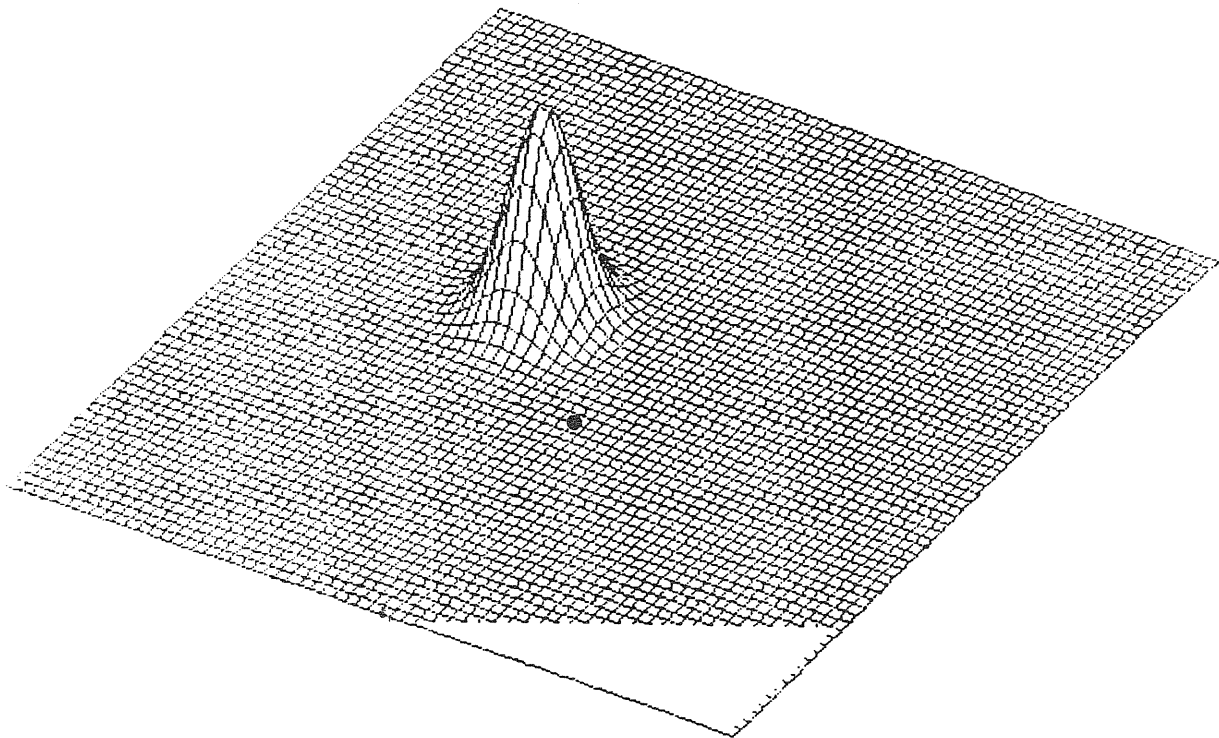


Fig. 4.2

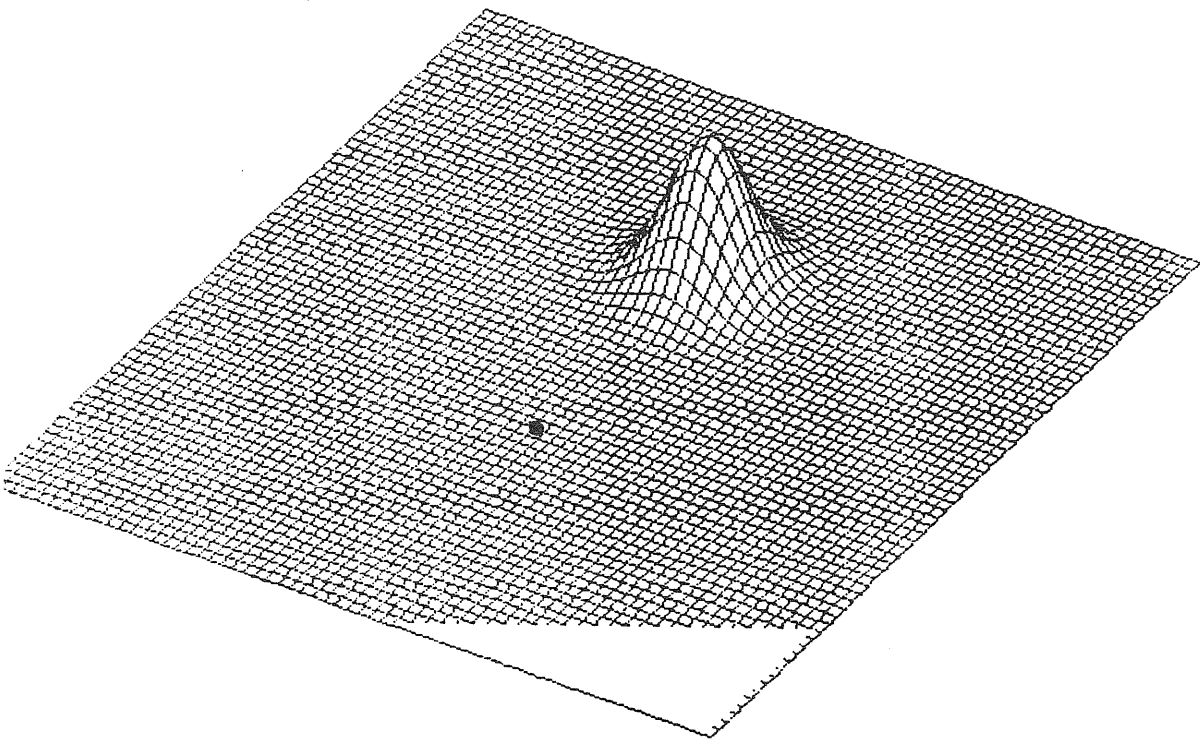


Fig. 4.3

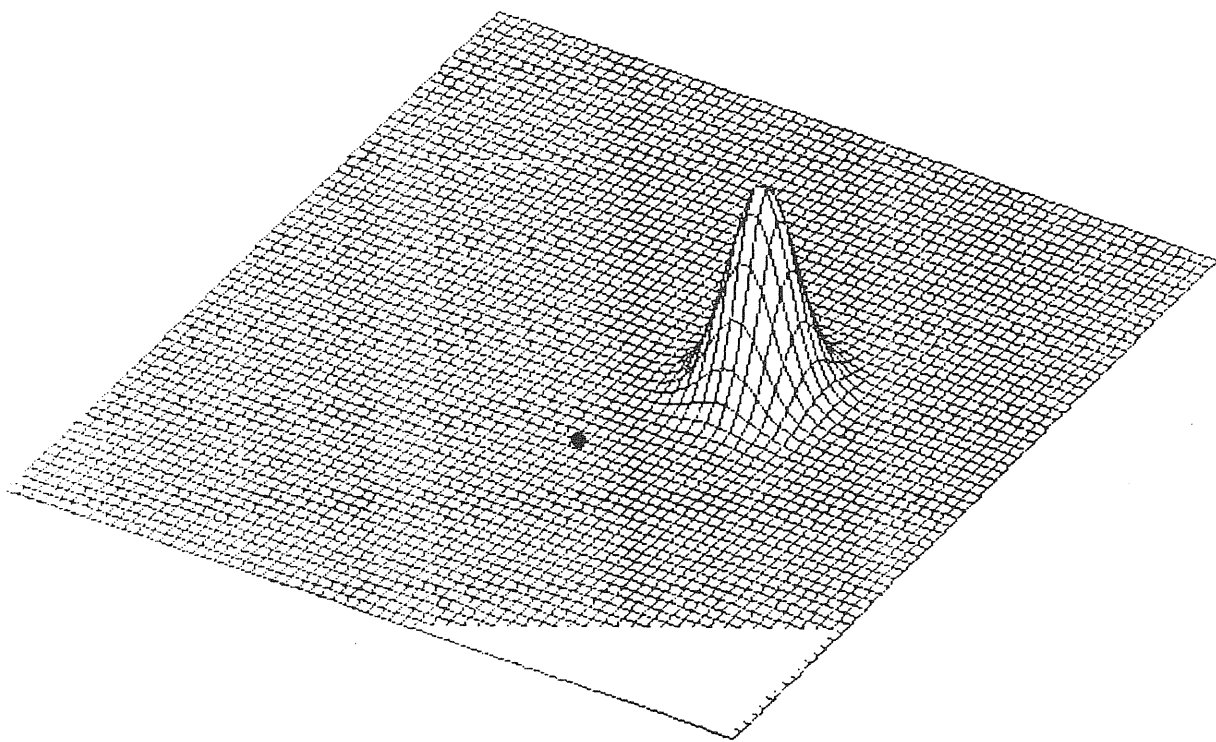


Fig. 4.4

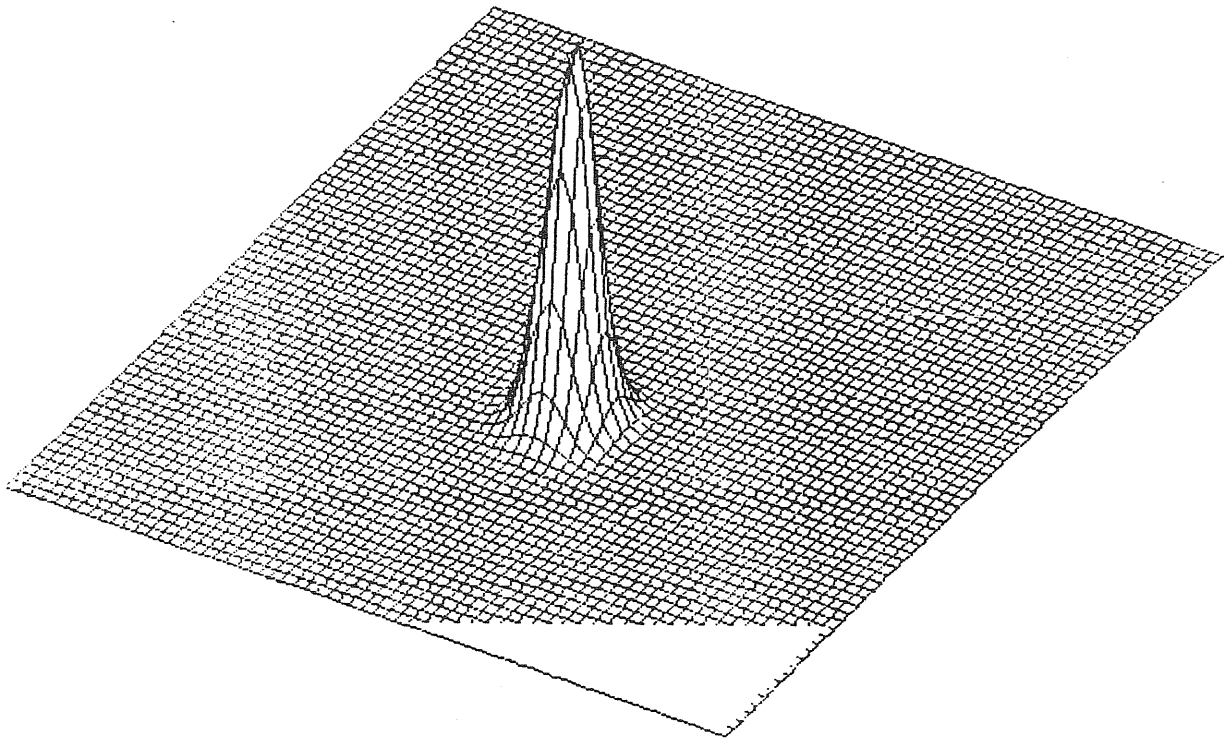


Fig. 4.5

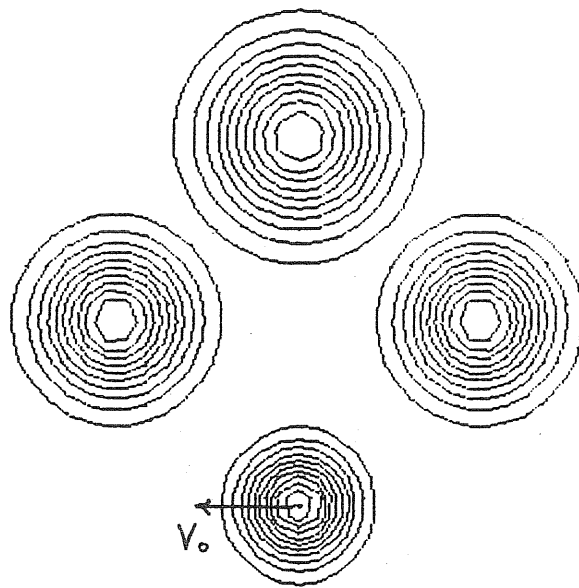


Fig. 4.6

Figs(4.1)-(4.6) The trajectory of a wavepacket in a magnetic field. The radius $R=750(\text{A})$. The Figs.(4.1)-(4.5) show the wavepacket at time $t = 0, T/4, T/2, 3T/4$ and T , respectively. Here $T = 2.39$ (picosecond) is the periodicity. The dark dot represents the initial position of the wavepacket. The Fig.(4.6) is the contour plot of the trajectory. The calculation is performed using SYMMETRY GAUGE in the conditions Magnetic field $B = 2$ (tesla) and initial velocity $V = 3908$ (A/ps). The width of wavepacket(141.44(A)) is smaller than magnetic length (181.44(A))

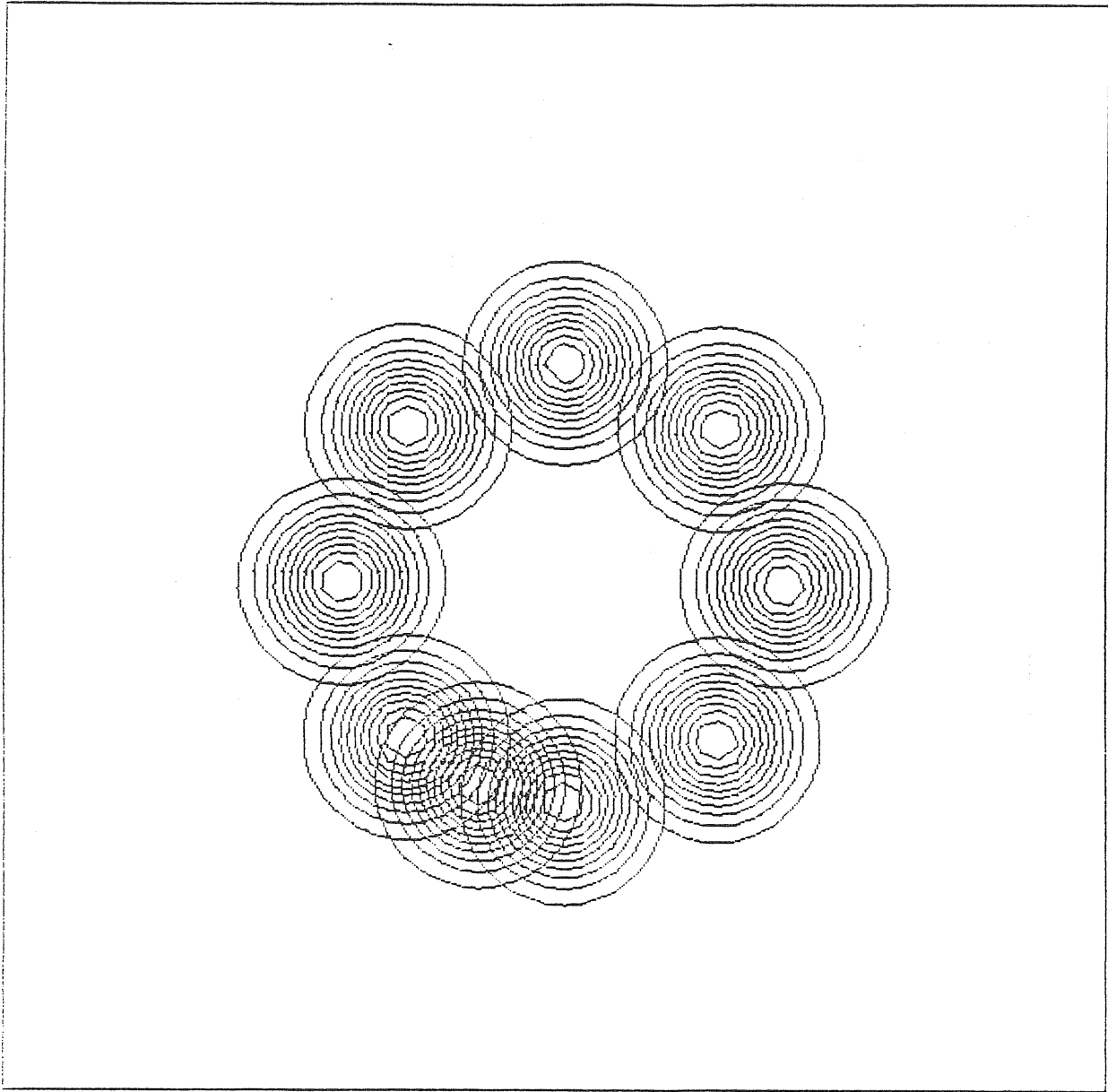


Fig. 4.7

Figs(4.7) The trajectory of a wavepacket in a magnetic field. The width of wavepacket(181.44(A)) is equal to magnetis length (181.44(A)). The shape does not change in the motion.

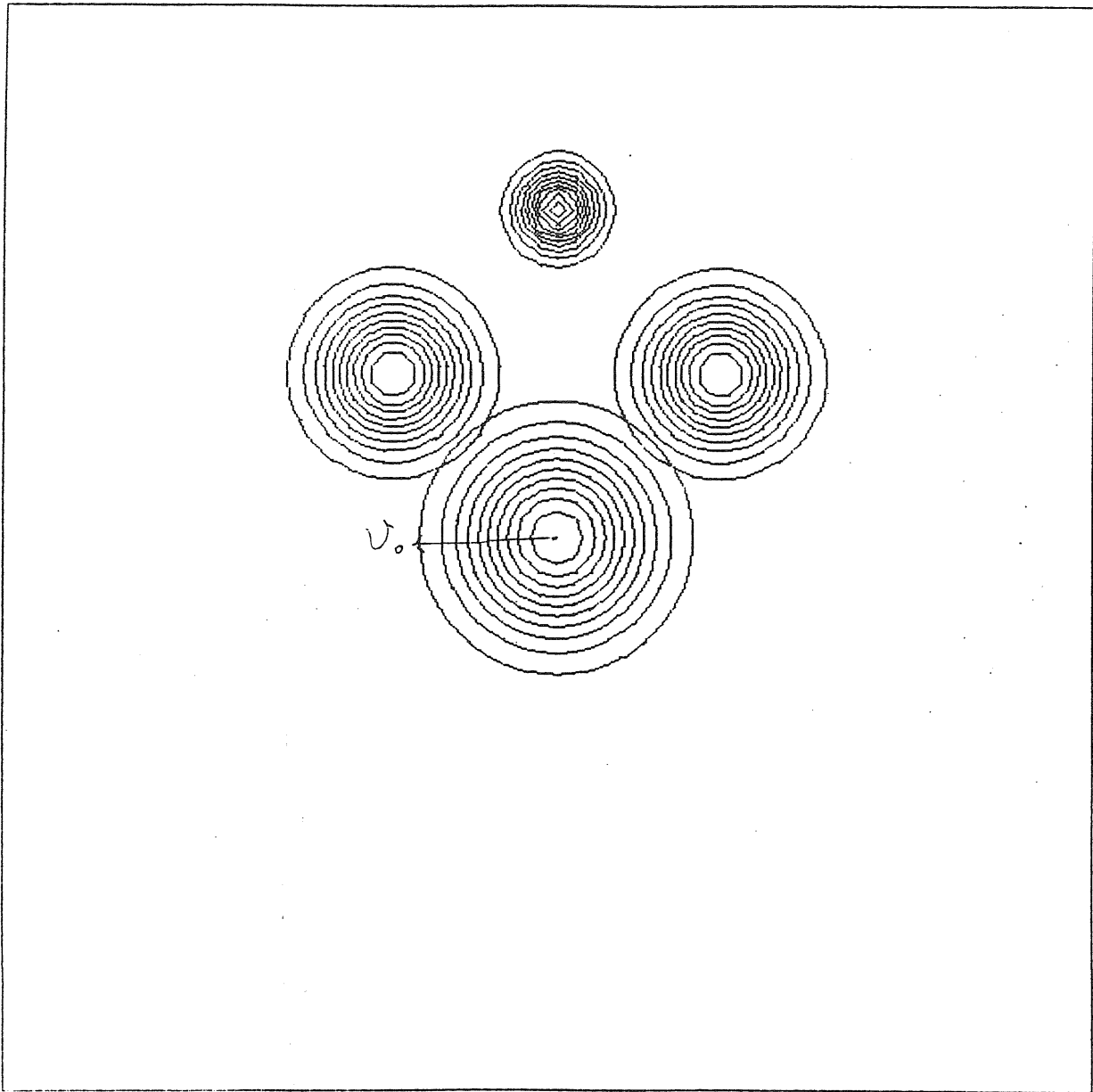


Fig. 4.8

Figs(4.8) The trajectory of a wavepacket in a magnetic field. The width of wavepacket(282.88(A)) is larger than magnetis length (181.44(A)). The wavepacket contracts in the first half periodicity and returns back to the original form.

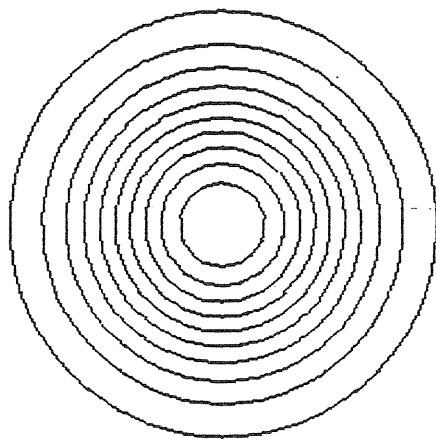


Fig. 4.9

Fig.(4.9) The free wavepacket propagation at time $T/2$. The wavepacket spreads much faster than in the case of presence of magnetic field. The initial wavepacket is the same as the initial wavepacket shown in Fig.(4.6).

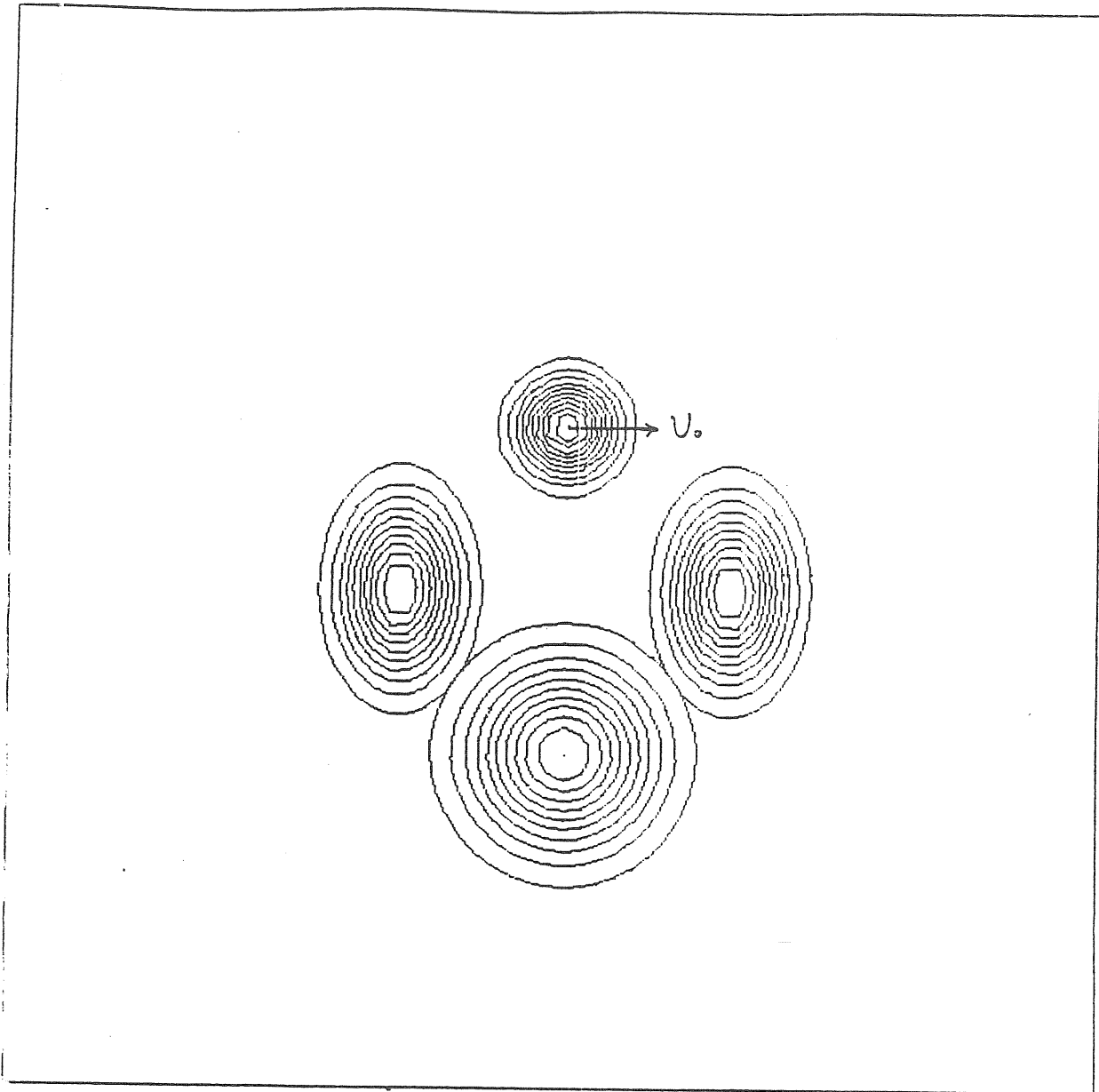


Fig. 4.10

Fig.(4.10) The trajectory of the wavepacket using the LANDAU GAUGE and same initial inputs as in Figs.(4.1)-(4.6). The trajectory is the same, but the shape of the wavepacket is different from the one in symmetry gauge. The initial density of the initial wavepacket in the two gauges is the same, but the internal current distributions differ.

Chapter 5

TUNNELING THROUGH A POTENTIAL BARRIER IN THE
PRESENCE OF A TRANSVERSE MAGNETIC FIELD

In chapter 4, we discussed the motion of a wavepacket in a magnetic field in the absence of potential barrier. In this chapter we shall present how a wavepacket tunnels through a potential barrier in a transverse magnetic field and show the motion of the reflected and transmitted parts of the wavepacket after tunneling. The geometry of the barrier with a magnetic field is shown in Fig.(1.1). This is the first step in our study of the tunneling problem. In the future we will calculate physical quantities such as transmission coefficients and transversal time versus magnetic field in order to compare with experiments and other theories.

The results are shown in Figs.(5.1)-(5.6). These were obtained using the numerical method described in chap.3, with a spatial grid of 128 by 128 points in a square of dimensions $L=8000(\text{A})$. The barrier height and width are $V=0.05(\text{eV})$ and $d=100(\text{A})$ respectively. The initial wavepacket is gaussian with radius $\sigma=200(\text{A})$, and the average energy is $E=\langle\psi|H|\psi\rangle=0.03(\text{eV})$. The calculations were performed using the Landau gauge. Initially the wavepacket moves along the cyclotron orbit. When it reaches the potential barrier, the wavepacket starts to strongly oscillate and many peaks appear in the region of the barrier.

Afterwards the wavepacket is separated into reflected and transmitted parts. The motion of mean positions of the reflected and transmitted parts look like that of two wavepackets in a magnetic field. However, the wavepackets appear to be strongly distorted with respect to the case when no barrier is present.

The transmission coefficient can be obtained by integrating the transmitted part of the wavepacket on the right side of the barrier (Suppose the initial wavepacket is normalized). One must be sure that the reflected and transmitted parts have completely separated. In Fig.(5.5) the transmitted part goes faster than in the case of absence of barrier. This fact depends on the fact that the transmitted part has a Fourier transform shifted to higher momenta. The radius of the motion of the transmitted part is larger than in absence of the barrier. According to the conservation of the momentum the reflected part contains lower momenta and the radius is smaller[16]. These points will be discussed in more detail in the future.

This is just the beginning of our study of tunneling in a transverse magnetic field. Many points will require further investigation.

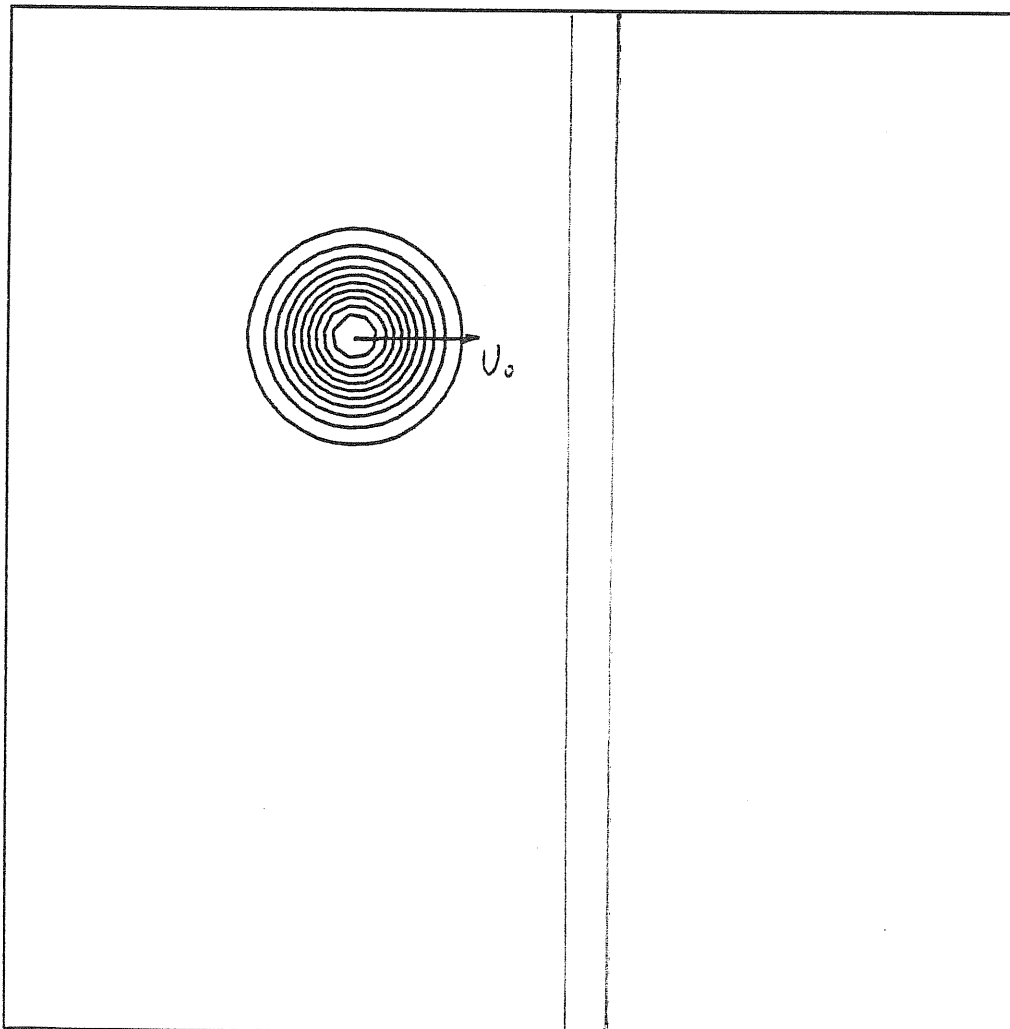
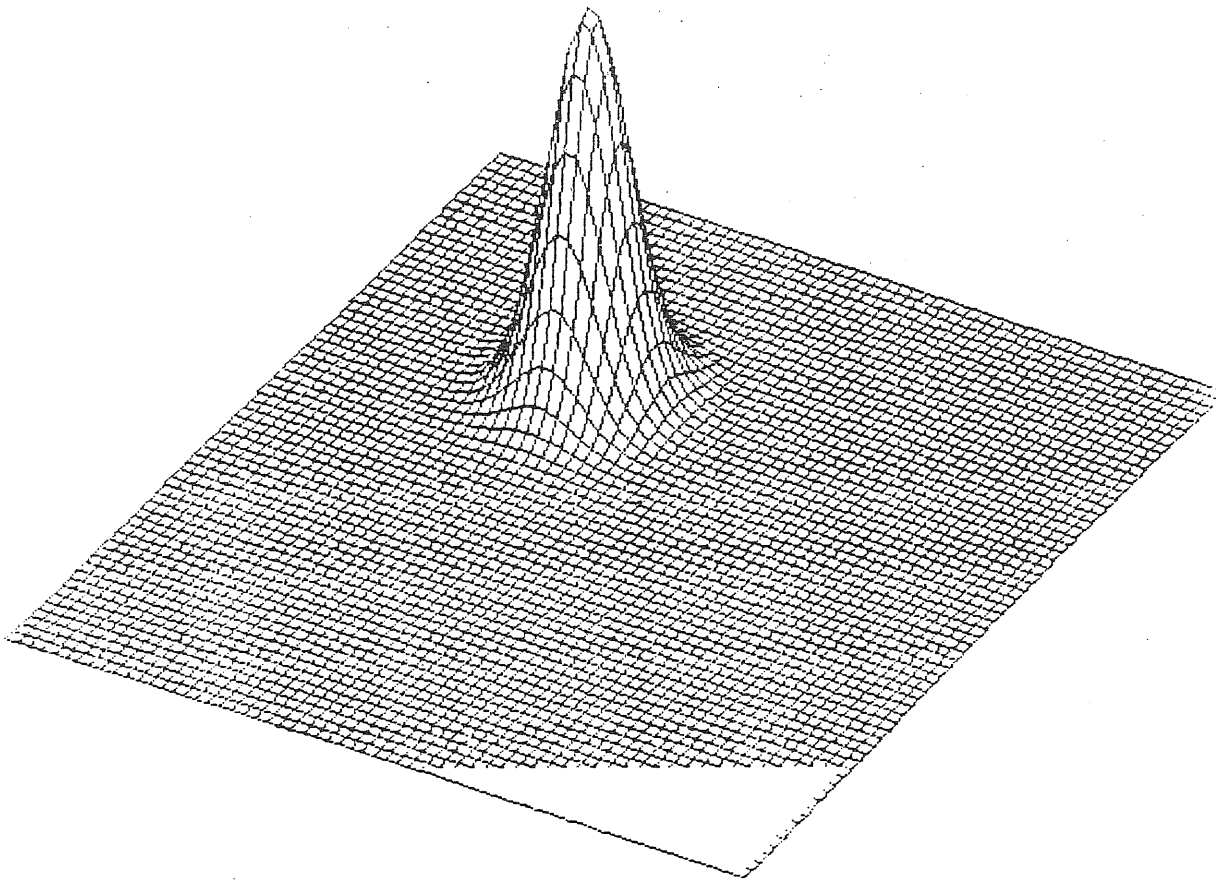


Fig. 5-1

max

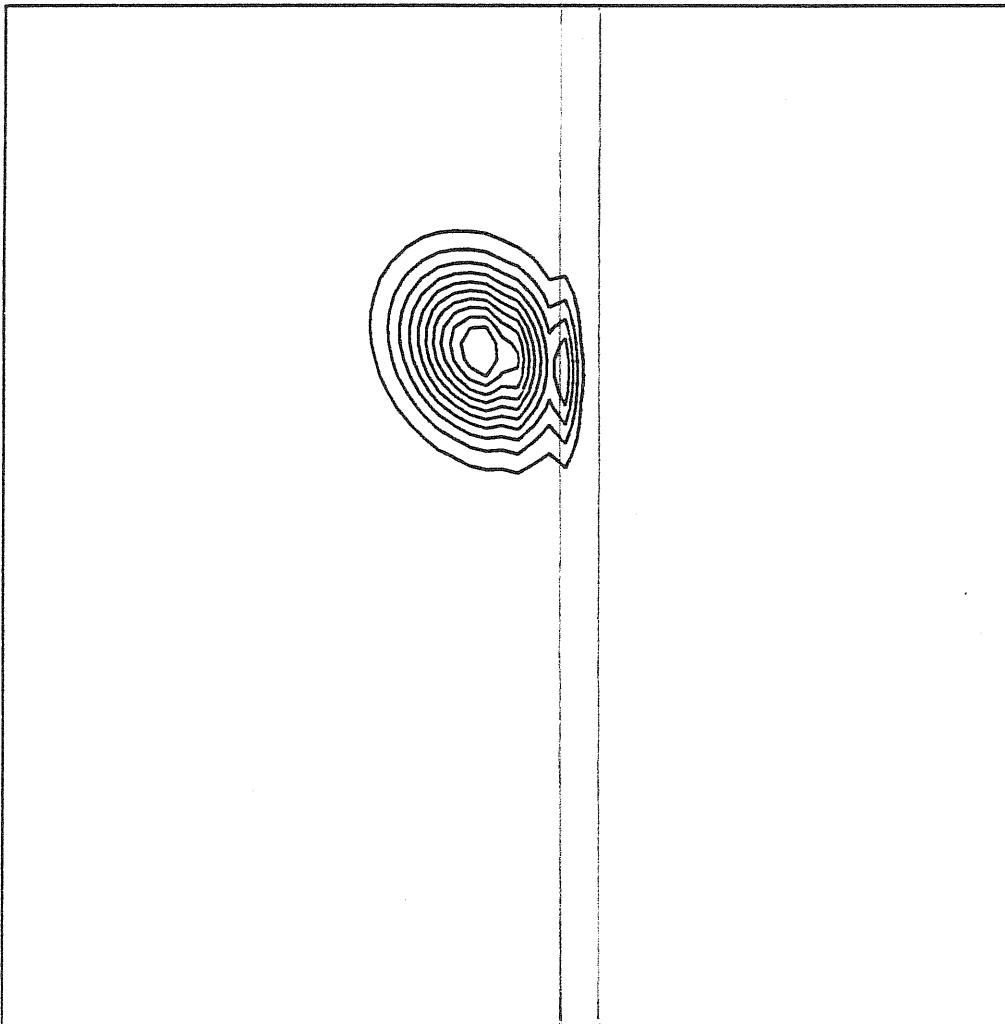
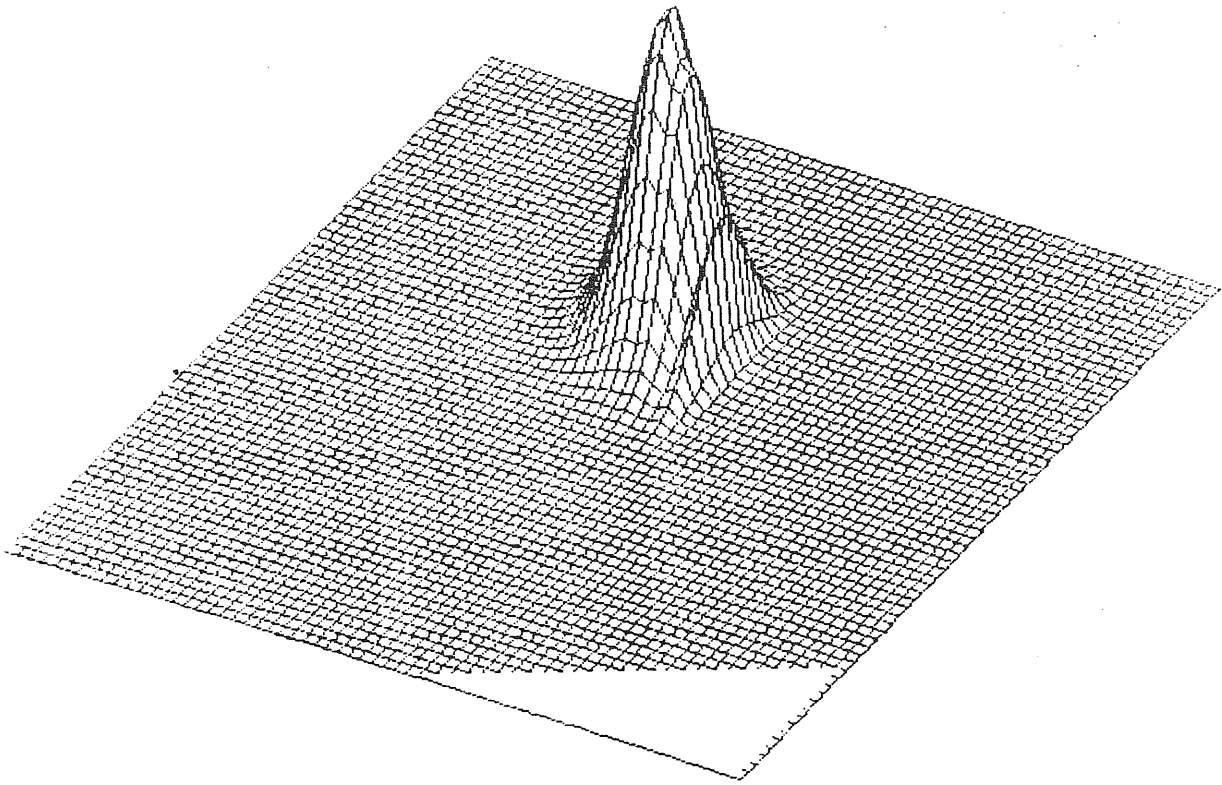


Fig. 5.2

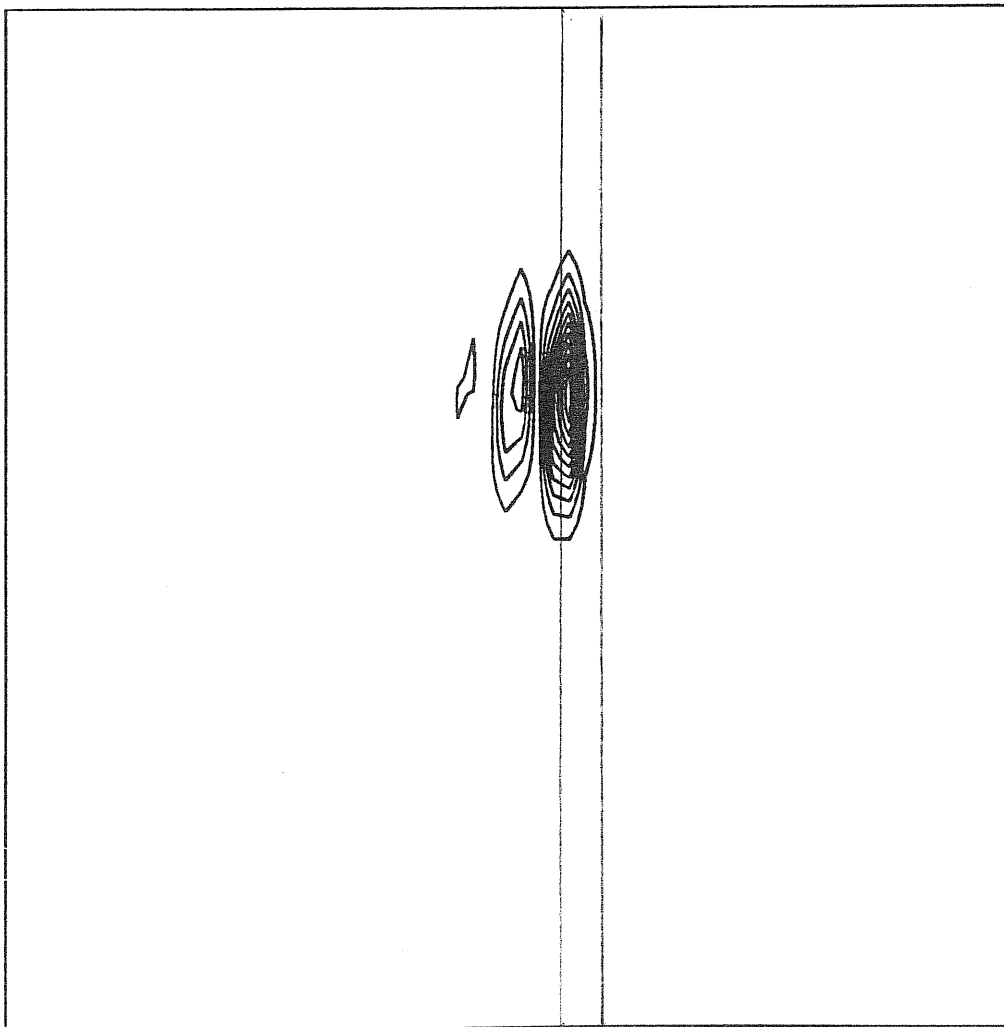
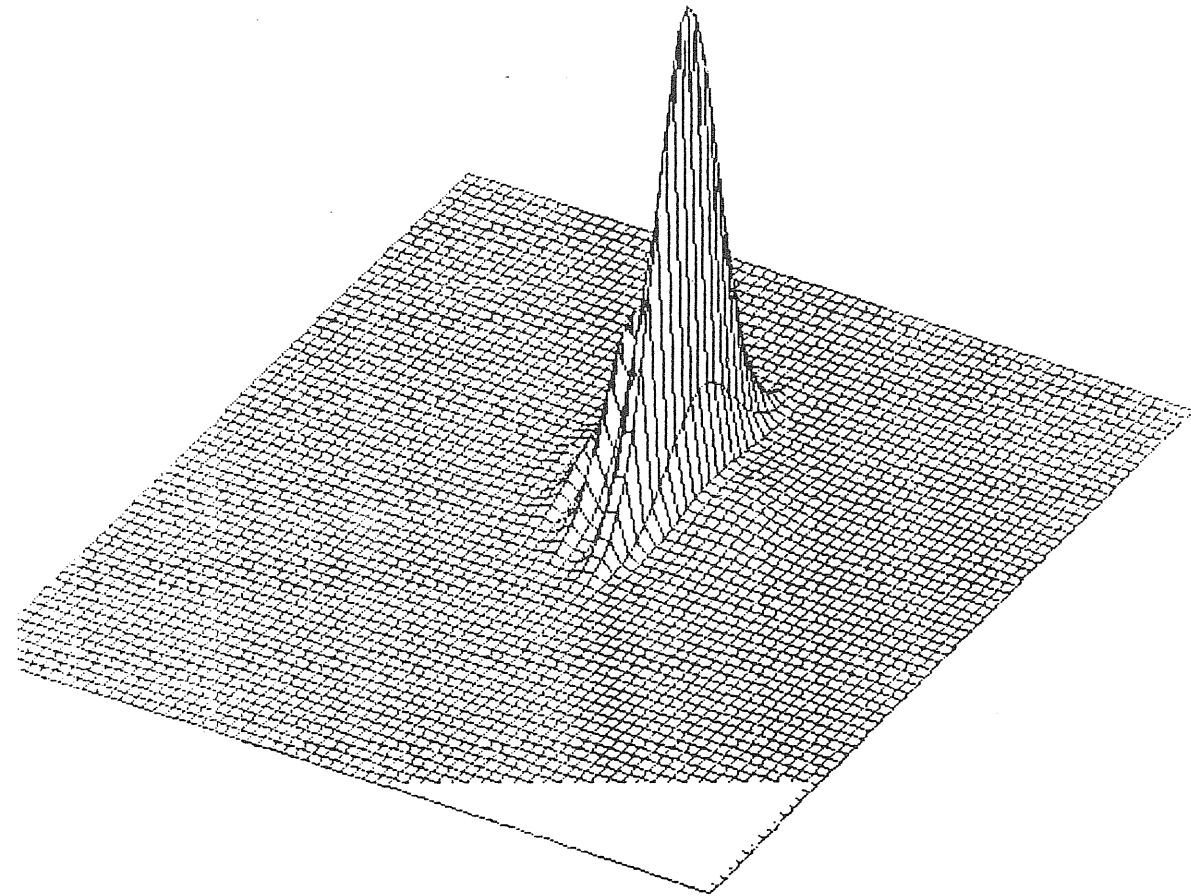


Fig. 5.3

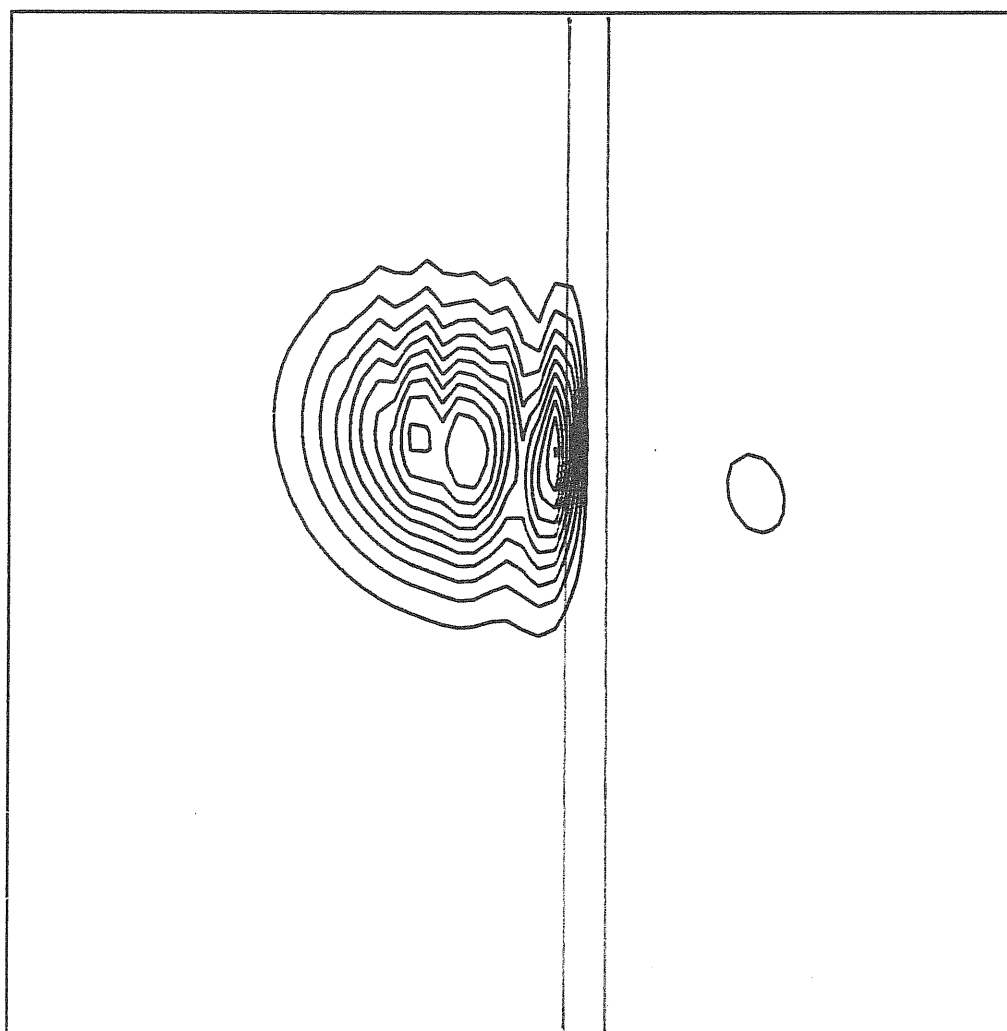
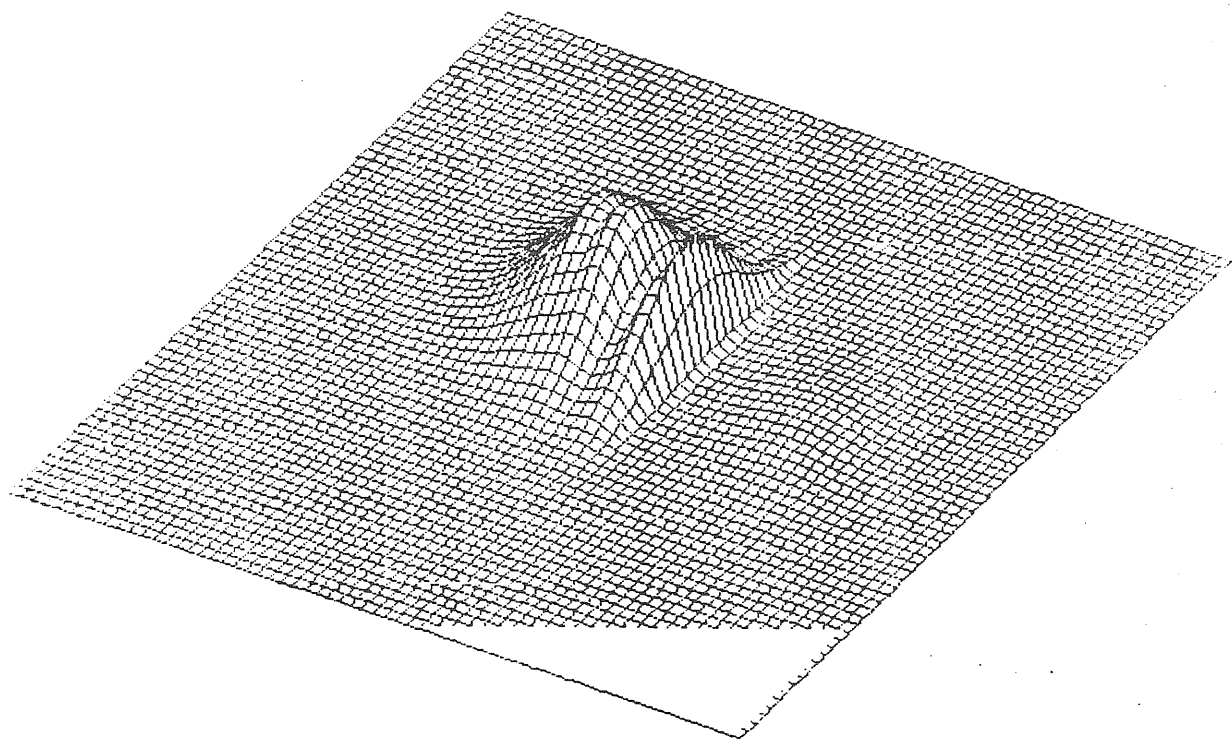


Fig. 5.4

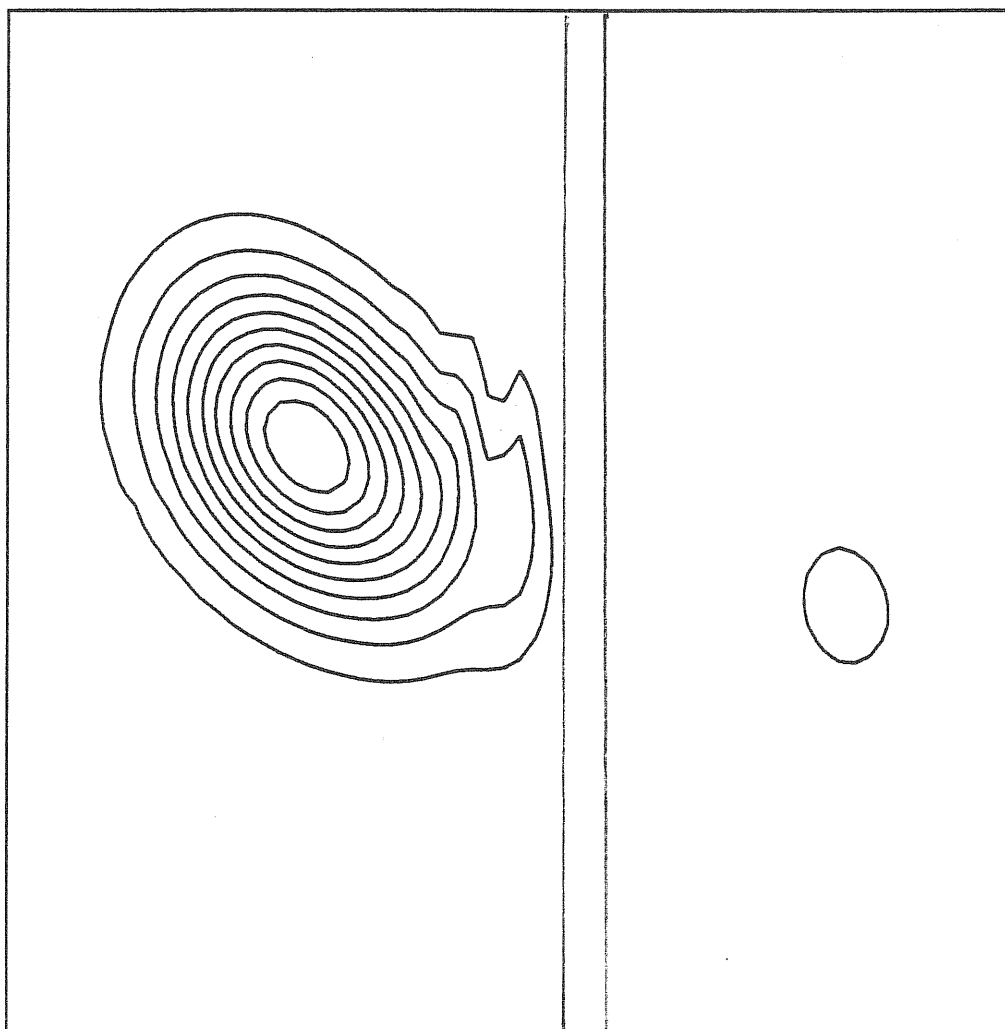
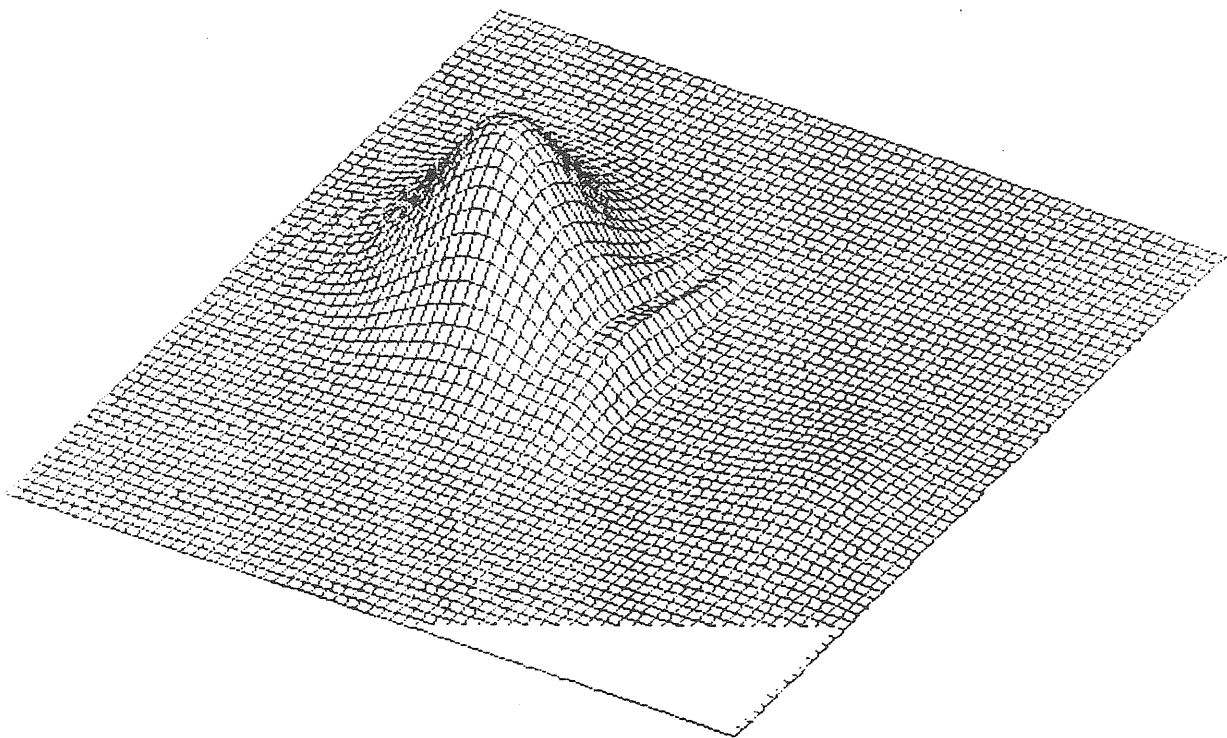


Fig. 5-5

Figs.(5.1)-(5.5) Wavepacket tunneling through a potential barrier in a transverse magnetic field. The figures show the wavepacket at time $t= 0, 0.1, 0.2, 0.3,$ and 0.4 (ps), respectively.

TUNNELING TRAJECTORY OF A WAVEPACKET

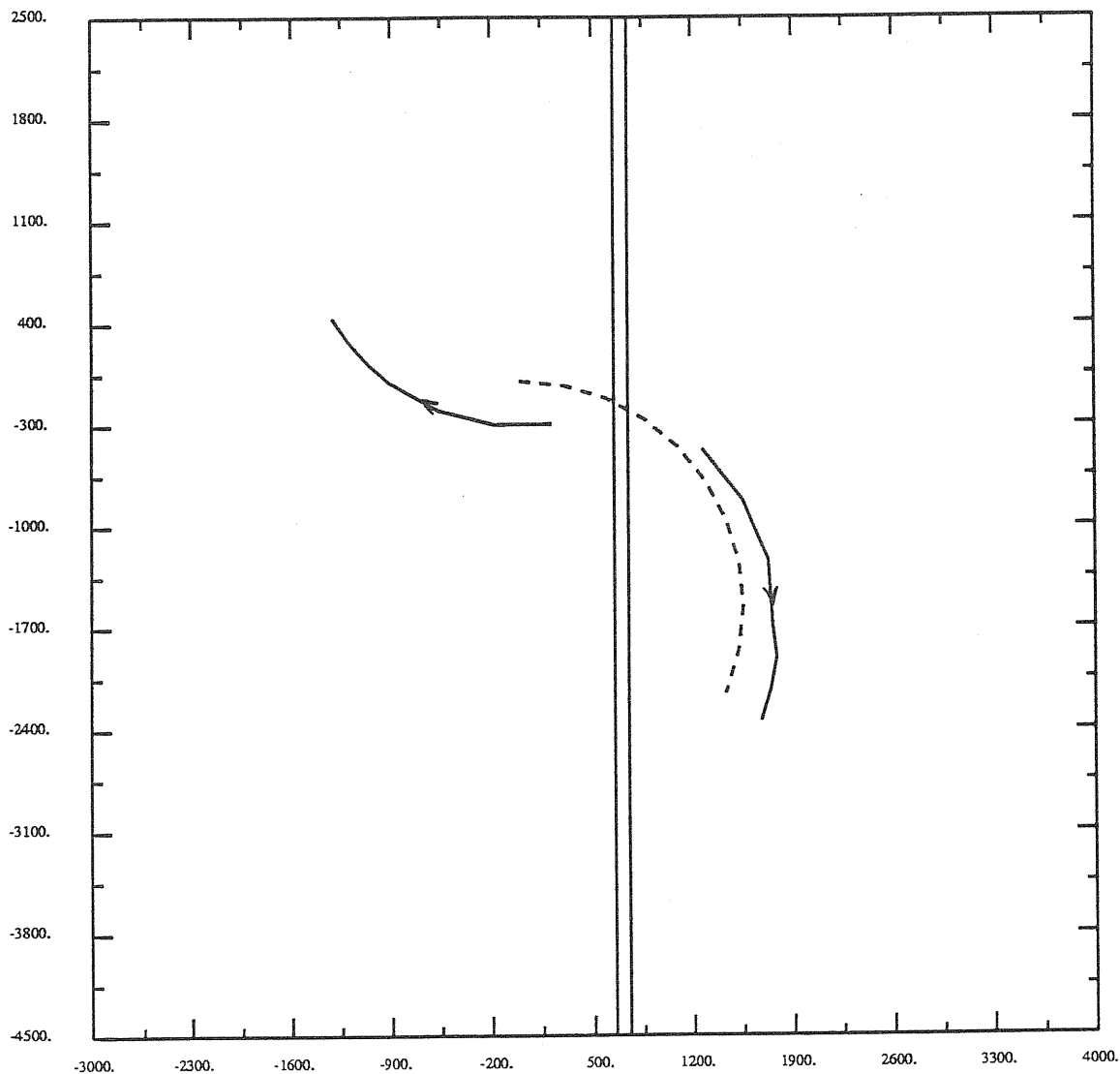


Fig. 5.6

Fig.(5.6) The trajectories of the reflected and transmitted parts after tunneling in a transverse magnetic field. In this case the transmitted part goes faster than in the absence of barrier (dashed curve).

Chapter 6

CONCLUSIONS

In this last chapter, we summarize the main results we have obtained in this thesis. These conclusions are only provisional and some of them require further investigation.

We are concerned with tunneling in the presence of a transverse magnetic field. We have solved numerically both the time-independent and time-dependent Schrodinger equations in the presence of a potential barrier and a magnetic field.

The results show that for the stationary case the Landau levels become strongly position dependent and oscillate. For a thin barrier the number of minima of the Landau levels corresponds to the number of the nodes of the wavefunction. However for a thick barrier the number of the minima of the Landau levels does not corresponds to the number of nodes of the wavefunction because the thick barrier influences both the nodes and extrema of the wavefunction simultaneously.

The time-dependent Schrodinger equation is solved by using the Chebychev polynomial expansion scheme, which is extremely accurate and useful, especially for propagation across a long time interval.

The results for the motion of a wavepacket in a magnetic field show interesting features. Generally the motion of a

wavepacket is periodic. The wavepacket turns back to the original position and shape in the time $T=2\pi/\omega_c$, where $\omega_c=eB/(mc)$ is the cyclotron frequency. The wavepacket center moves along the cyclotron orbit as expected, The width of wavepacket changes also periodically in a way which depends upon the magnetic field.

In a weak magnetic field, if the magnetic length $L_B = (hc/(eB))^{1/2}$ is larger than the width σ_x of the initial wavepacket, the wavepacket spreads out for time $t < T/2$ (although less than the free wavepacket propagation) and then compresses back to its original form for $T/2 < t < T$. If the magnetic length L_B is equal to the width of the wavepacket σ_x , the wavepacket keeps its shape during the motion. Finally if the magnetic field is so strong that the magnetic length L_B is smaller than the σ_x , the wavepacket contracts in the first half period and expands back to the initial form in the second half. In summary wavepacket is confined by the magnetic field. The confinement becomes stronger with increasing magnetic field. These properties are independent of the velocity of wavepacket and remain true in the case of wavepackets with zero velocity. The mean position of wavepacket does not change in time, while the shape of wavepacket changes periodically as described.

Lastly we show how a wavepacket tunnels through a potential barrier in a transverse magnetic field and study the motion of the reflected and transmitted parts of the wavepacket after tunneling. The wavepacket is strongly scattered by the potential barrier, and separate into a reflected part and a transmitted part. The trajectories of these two parts are arcs of circular orbit as well. We plan to calculate other physical quantities such as transmission coefficients and transversal time versus magnetic field in the future.

REFERENCES

- 1.) See some standard textbooks, for example, L.I.Schiff, <<QUANTUM MECHANICS>>, McGraw-Hill Book Company, 1968.
- 2.) K.W.H.Stevens, European J. Phys., 1(1980)98; J. Phys. C, 16(1983)3694.
- 3.) M. Buttiker and R. Landauer, Phys. Rev. Lett., 49(1982)1739.
- 4.) L. Eaves, D.C. Taylor, J.C. Portal, and L. Dmowski, Two-Dimensional Systems, Heterostructures, and Superlattices, edited by G. Bauer, F. Kuchar, and H. Heinrich, Springer(1986).
- 5.) P. Gueret, A. Baratoff, and E. Marclay, Europhys. Lett., 3(1987)367.
- 6.) E.O.Kane, Tunneling Phenomena in Solids, edited by E.Burnstein and S. Lundquist (Plenum, New York, 1969), Chap.1.
- 7.) C.B. Duke, Tunneling in solids, (Academic, New York, 1969).
- 8.) R.B. Gerber, R. Kosloff, and M. Berman, Comp. Phys. Rep. 5(1986)59.
- 9.) L.D. Landau and E.M. Lifshitz, <<Quantum Mechanics>>, Chap.15.
- 10.) F.Herman and S. Skillmman, Atomic Structure calculations (Prentice-Hall, Englewood Cliffs, N. J., 1963).
- 11.) P.C. Chow, Amer. J. Phys., 40(1972)730.

- 12.) H. Tal-Ezer, R. Kosloff, J. Chem. Phys. 81(9) (1984)3967.
- 13.) C. Temperton, J. Comp. Phys. 52(1983)1.
- 14.) H.J. Nussbaumer, Fast Fourier Transform and Convolution Algorithms, 2nd ed. (Springer, Berlin, 1982).
- 15.) A. Messiah, <<Quantum Mechanics>>, Amsterdam, North-Holland, 1961, Chap.6.
- 16.) M. Buttiker, Phys. Rev. B, 27(1983)6178.